SUPPORTING INFORMATION

P,N-type phosphaalkene-based Ir(I) complexes: synthesis, coordination chemistry, and catalytic applications

Priyanka Gupta,[a,b] Hans-Joachim Drexler,[a] Richard Wingad,[b] Duncan Wass,[b] Eszter Baráth,[a] Torsten Beweries[a] and Christian Hering-Junghans*[a]*

[a]Leibniz-Institut für Katalyse e.V. (LIKAT), Albert-Einstein Straße 29a, 18059 Rostock, Germany. E-mail: torsten.beweries@catalysis.de, christian.hering-junghans@catalysis.de

[b]Cardiff Catalysis Institute, Cardiff University, Translational Research Hub, Maindy Road, Cathays, Cardiff, Wales, CF24 4HQ

This file includes:

1   EXPERIMENTAL

General Information. If not stated otherwise, all manipulations were performed under oxygen- and moisture-free conditions under an inert atmosphere of argon using standard Schlenk techniques or an inert atmosphere glovebox (MBraun LABstar ECO). All glassware was heated three times *in vacuo* using a heat gun and cooled under argon atmosphere. Solvents were transferred using syringes, steel- or PE-cannulas, which were purged with argon prior to use. Solvents and reactants were either obtained from commercial sources or synthesised as detailed in Table S1.

Table S1. Origin and purification of solvents and reactants.

Substance	Origin	Purification
Benzene	local trade	dried over Na/benzophenone freshly distilled prior to use, stored over molecular sieves
CH_2Cl_2	local trade	purified with the Grubbs-type column system "Pure Solv MD-5", stored over molecular sieves
n-pentane, *n*-hexane	local trade	dried over Na/benzophenone/tetraglyme freshly distilled prior to use
Toluene	Fisher Chemical, for HPLC	purified with the Grubbs-type column system "Pure Solv MD-5"
Pyrdine	Acros organics	dried over P_4O_{10} and CaH_2 freshly distilled prior to use
THF	local trade	purified with the Grubbs-type column system "Pure Solv MD-5", stored over molecular sieves
PhF	local trade	dried over CaH_2 freshly distilled prior to use
CD_2Cl_2	euriso-top	dried over P_4O_{10} and CaH_2 freshly distilled prior to use
CD_3CN	euriso-top	degassed using multiple freeze-pump-thaw cycles and stored over molecular sieves

Substance	Origin	Purification
Benzene	local trade	dried over Na/benzophenone freshly distilled prior to use, stored over molecular sieves
THF-d_8	Sigma-Aldrich	degassed using multiple freeze-pump-thaw cycles and stored over molecular sieves
quin-CH=PMes*[1]	Synthesised	
$[Ir(coe)_2(Cl)]_2$	Sigma-Aldrich	used as received
AgOTf	Abcr chemical	used as received
4-Dimethylaminopyridine	Aldrich	used as received
$NaBF_4$	Sigma-Aldrich	used as received
$(CH_3)_2Mg$[2]	Synthesised	
NaN_3	Sigma-Aldrich	used as received
LiCl	Sigma-Aldrich	used as received

NMR spectra were recorded on Bruker spectrometers (AVANCE 300, AVANCE 400 or Fourier 300) and were referenced internally to the deuterated solvent ($^{13}C\{^1H\}$: CD_2Cl_2 δ_{ref} = 54.0 ppm; C_6D_6 δ_{ref} = 128.06 ppm; C_7D_8 δ_{ref} = 137.86 ppm) or to protic impurities in the deuterated solvent (^1H: $CHDCl_2$ δ_{ref} = 5.32 ppm; C_6HD_5 δ_{ref} = 7.16 ppm; C_7HD_7 δ_{ref} = 2.09 ppm). All measurements were carried out at ambient temperature unless denoted otherwise. NMR signals were assigned using experimental data (e.g., chemical shifts, coupling constants, integrals where applicable).

IR spectra of crystalline samples were recorded on a Bruker Alpha II FT-IR spectrometer equipped with an ATR unit at ambient temperature under argon atmosphere. Relative intensities are reported according to the following intervals: weak (w, 0–33%), medium (m, 33–66%), strong (s, 66–100%).

Elemental analyses were obtained using a Leco Tru Spec elemental analyser.

Mass spectra were recorded on a Thermo Electron MAT 95-XP sector field mass spectrometer using crystalline samples.

UV/Vis spectra were acquired on an Agilent Technologies Cary 60 UV-Vis spectrometer and on a METTLER TOLEDO UV-Vis-Excellence UV5 spectrometer.

GC analysis of all ethanol/methanol coupling reaction samples was performed by GC-FID, using an Agilent 7820A GC, fitted with a carbowax capillary column, 30 m x 0.32 mm, I.D. 0.25 μm. Method: starting oven temp 60 °C, hold at 60 °C for 5 min, heat to 220 °C at 40 °C min^{-1}, hold at 220 °C for 5 min.

2   STRUCTURE ELUCIDATION

X-ray Structure Determination

X-ray quality crystals were selected in Fomblin YR-1800 perfluoroether (Alfa Aesar) at low temperature. Diffraction data were collected at 123(2) K on a Bruker Kappa APEX II Duo diffractometer using Mo-K$_\alpha$ radiation **5** and **10** or Cu-K$_\alpha$ radiation **6**. The structures were solved by iterative (SHELXT)[3] or direct methods (SHELXS-97)[4] and refined by full matrix least square techniques against F^2 (SHELXL-2014)[5]. Semi-empirical absorption corrections were applied (SADABS/Bruker).[6] The non-hydrogen atoms were refined anisotropically. The hydrogen atoms were placed into theoretical positions and were refined by using the riding model. Contributions of solvent molecules were removed in **6** from the diffraction data with PLATON/SQUEEZE.[7] DIAMOND (Crystal Impact GbR) was used for structure representations.

Crystallographic data (excluding structure factors) for the structures reported in this paper have been deposited at the Cambridge Crystallographic Data Centre. Copies of the data can be obtained free of charge on application to CCDC, 12 Union Road, Cambridge, CB21EZ, UK (fax: int. code + (1223) 336-033; e-mail: deposit@ccdc.cam.ac.uk

Table S2. Crystallographic details of **5**, **6**, and **10**.

| Compound	5	6	10
Chem. Formula	$C_{54}H_{74}Cl_3IrN_2P_2 \cdot CH_2Cl_2$	$C_{62}H_{77}F_3IrN_3O_3P_2S$	$C_{57}H_{75}IrN_2P_2 \cdot CH_2Cl_2$
Formula weight [g/mol]	1149.68	1255.46	1127.25
Colour	dark blue	blue	dark blue
Crystal system	triclinic	monoclinic	triclinic
Space group	$P\bar{1}$	$C2/c$	$P\bar{1}$
a [Å]	11.1077(6)	34.913(4)	11.0126(5)
b [Å]	16.1595(9)	14.0591(16)	16.1820(7)
c [Å]	16.8165(9)	26.445(3)	16.9882(10)
α [°]	64.569(2)	90	64.9570(10)
β [°]	80.492(2)	107.341(9)	80.310(2)
γ [°]	89.426(2)	90	89.453(2)
V [Å^3]	2682.3(3)	12391(3)	2697.2(2)
Z	2	8	2
$\rho_{calcd.}$ [g/cm^3]	1.424	1.346	1.388
μ [mm^{-1}]	2.736	5.403	2.672
T [K]	150	150	150
Measured reflections	52315	43683	142400
Independent reflections	10008	10165	13041
Reflections with $I > 2\sigma(I)$	8672	7779	12290
R_{int}	0.0571	0.0785	0.0271
$F(000)$	1180	5152	1160
$R_1(R[F^2>2\sigma(F^2)])$	0.0296	0.0491	0.0221
$wR_2(F^2)$	0.0728	0.1375	0.0578
GooF	1.048	1.012	1.075
No. of Parameters	635	788	635
CCDC #	2235638	2235639	2235640

3   SYNTHETIC PROCEDURES

3.1. Synthesis of [(Mes*P=CH-2-quin)$_2$IrCl] (5)
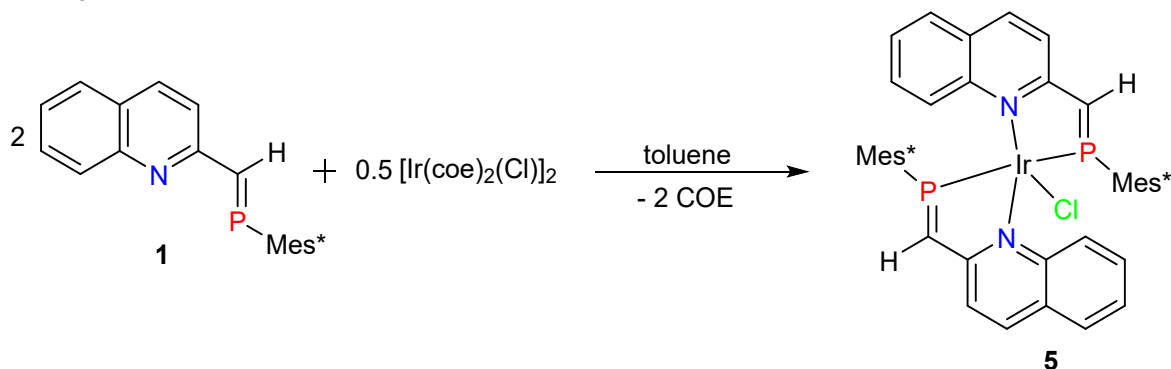

Compound **1** (0.251 g, 0.601 mmol) and [Ir(coe)$_2$(Cl)]$_2$ (0.134 g, 0.150 mmol) were combined in a Schlenk flask and dissolved in toluene (6 mL). Upon stirring the reaction mixture for 2 h at room temperature, a dark blue solid (complex **5**) precipitated from the reaction mixture. The mixture was then filtered inside the glove box using a frit and washed with *n*-pentane to obtain complex [(Mes*P=CH-2-quin)$_2$IrCl] (**5**, 0.215 g, 0.202 mmol, 67%) as analytically pure solid. X-ray quality crystals of **5** were grown from a saturated CH$_2$Cl$_2$ solution at −30 °C.

¹H NMR (300 MHz, CD$_2$Cl$_2$) δ [ppm] = 0.94 (s, 18H, C(C*H$_3$*)$_3$), 1.20 (s, 18H, C(C*H$_3$*)$_3$), 1.76 (s, 18H, C(C*H$_3$*)$_3$), 6.99 (br, 2H, Ar-*H*), 7.01 – 7.10 (m, 2H, Ar-*H*), 7.11 – 7.26 (m, 4H, Ar-*H*), 7.32 (d, J_{HH} = 8.7 Hz, 2H, Ar-*H*), 7.47 (d, J_{HH} = 8.5 Hz, 4H, Ar-*H*), 7.87 (t, J_{PH} = 2.9 Hz, 2H, C*H*=P), 9.78 (d, J_{HH} = 8.8 Hz, 2H, Ar-*H*). **³¹P{¹H} NMR** (122 MHz, CD$_2$Cl$_2$) δ [ppm] = 250.8. **¹³C{¹H} NMR** (101 MHz, CD$_2$Cl$_2$) δ [ppm] = 31.2 (C(C*H$_3$*)$_3$), 33.0 (C(C*H$_3$*)$_3$), 33.9 (C(C*H$_3$*)$_3$), 35.1 (*C*Me$_3$), 38.5 (*C*Me$_3$), 40.3 (*C*Me$_3$), 119.1 (Ar), 122.7 (Ar), 123.6 (Ar), 123.9 (Ar), 125.6 (Ar), 126.2 (Ar), 128.2 (Ar), 128.5 (Ar), 128.8 (br, P=C), 129.3 (Ar), 129.4 (Ar), 136.0 (Ar), 138.3 (Ar), 149.7 (Ar), 152.8 (Ar), 154.1 (Ar), 155.2 (Ar), 171.3 (Ar). **IR** (ATR, 32 scans, cm⁻¹): 2949 (m), 2904 (w), 2865 (w), 1603 (w), 1549 (w), 1505 (w), 1461 (w), 1447 (w), 1425 (m), 1392 (w), 1347 (s), 1329 (m), 1285 (w), 1236 (w), 1211 (w), 1177 (w), 1148 (w), 1122 (m), 1029 (w), 982 (w), 939 (s), 875 (w), 818 (m), 772 (w), 748 (m), 728 (m), 693 (w), 672 (w), 648 (w), 635 (w), 615 (w), 533 (w), 522 (w), 512 (w), 495 (w), 482 (m), 465 (w). **MS** (ESI-TOF): [M]⁺ expected: m/z = 1027.4823; found: m/z = 1027.4844. **Elemental analysis** for C$_{56}$H$_{72}$N$_2$P$_2$IrCl: C, 63.29; H, 6.83; N, 2.64 Found: C, 63.75; H, 7.26; N, 2.17.
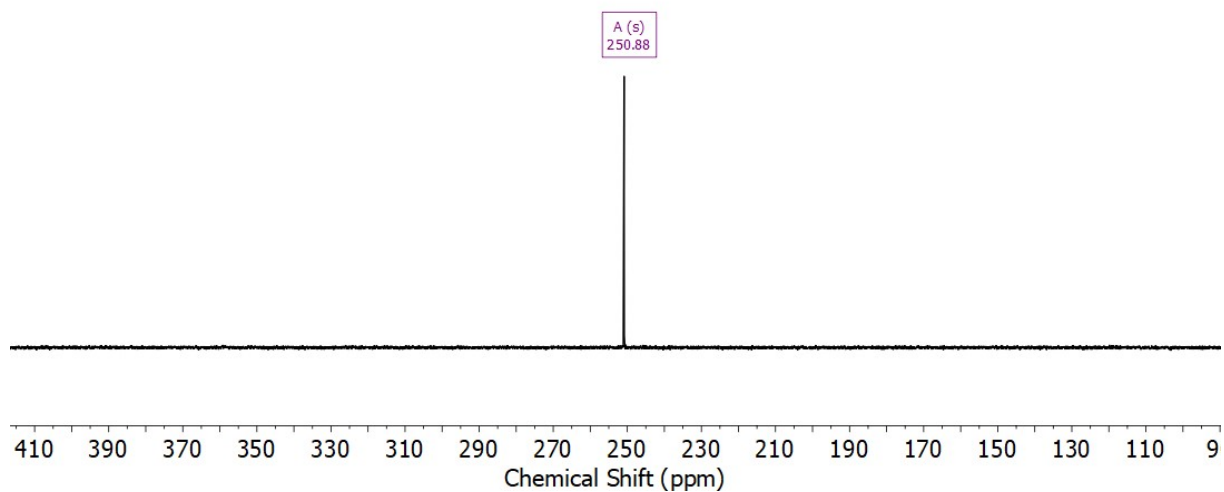
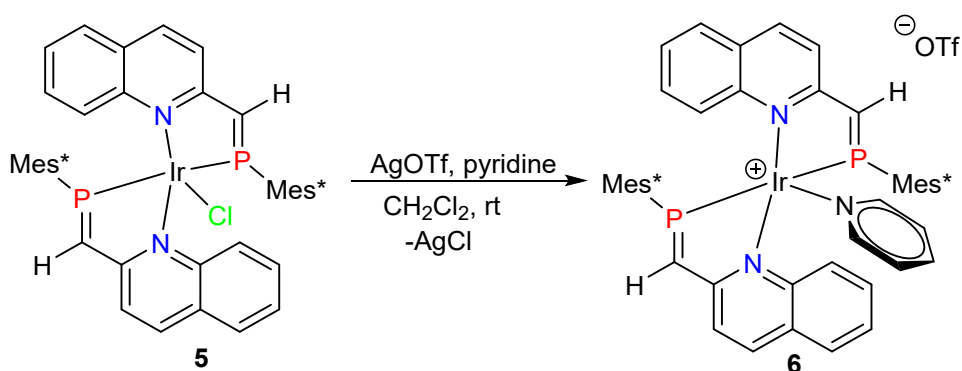**Figure S1.** $^{31}P\{^1H\}$ NMR spectrum of **5** (CD$_2$Cl$_2$, 122 MHz, rt).
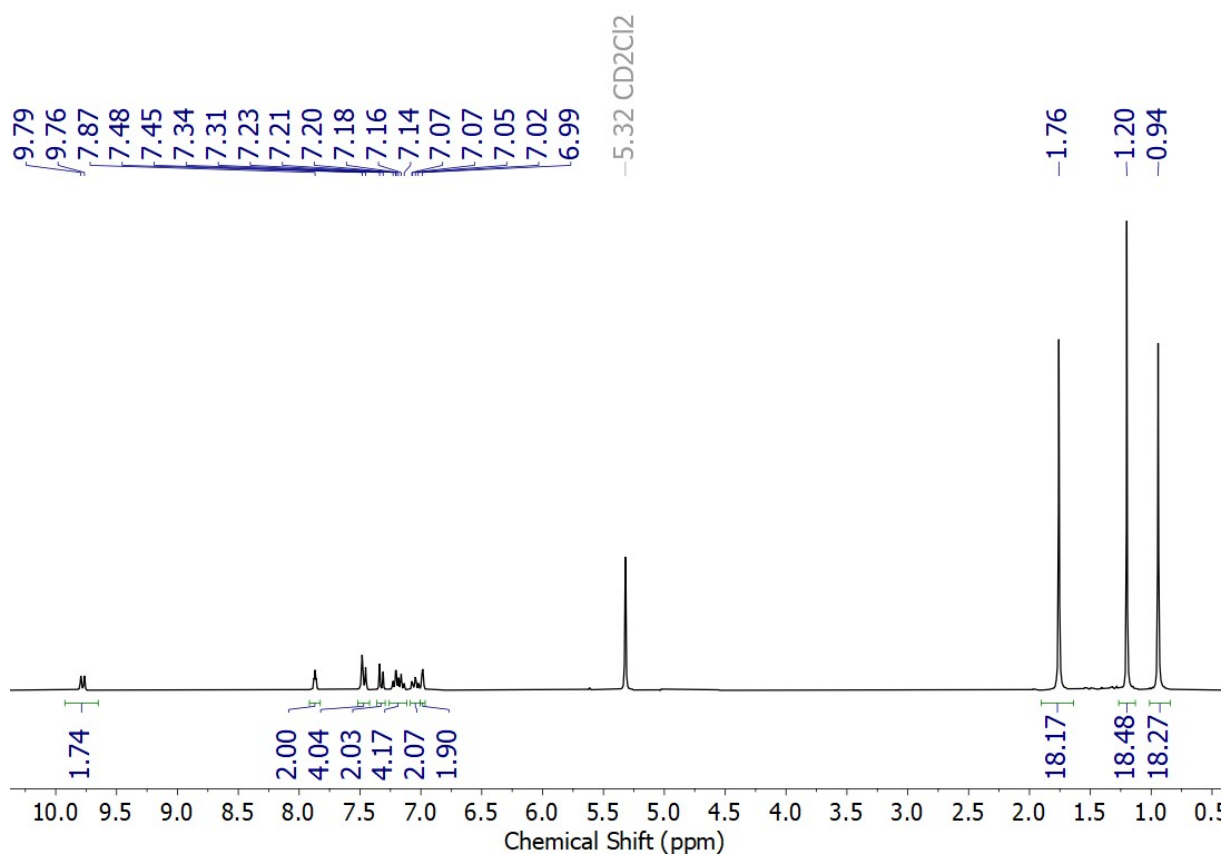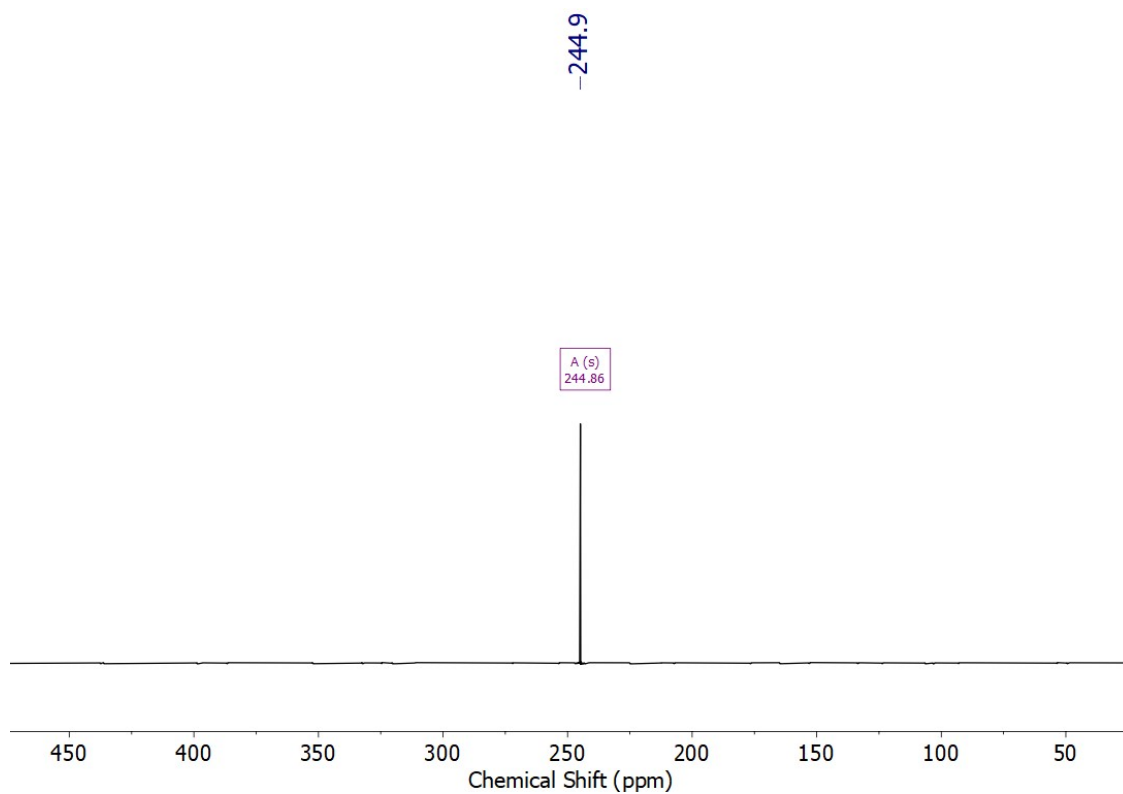

Figure S2. ^1H NMR spectrum of **5** (CD$_2$Cl$_2$, 300 MHz, rt).
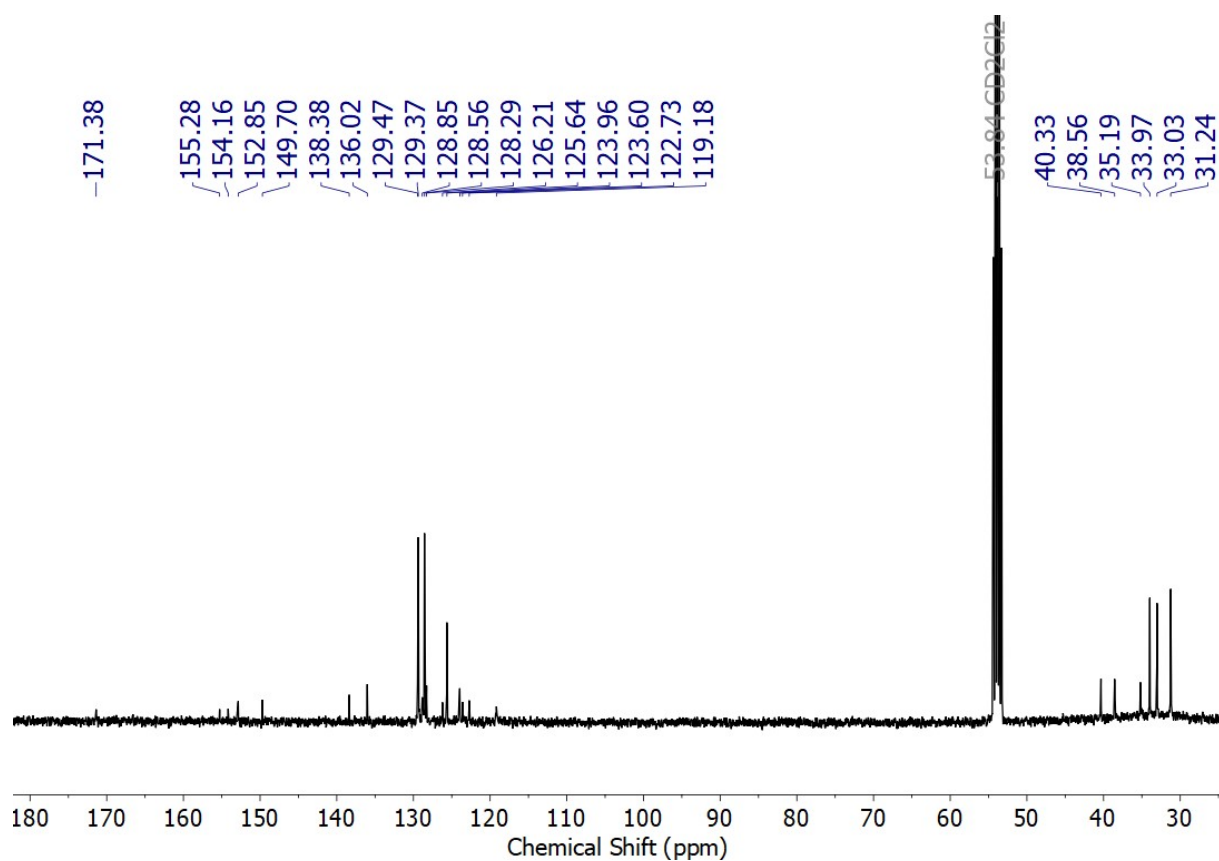
Figure S3. $^{13}C\{^1H\}$ NMR spectrum of **5** (CD$_2$Cl$_2$, 101 MHz, rt).

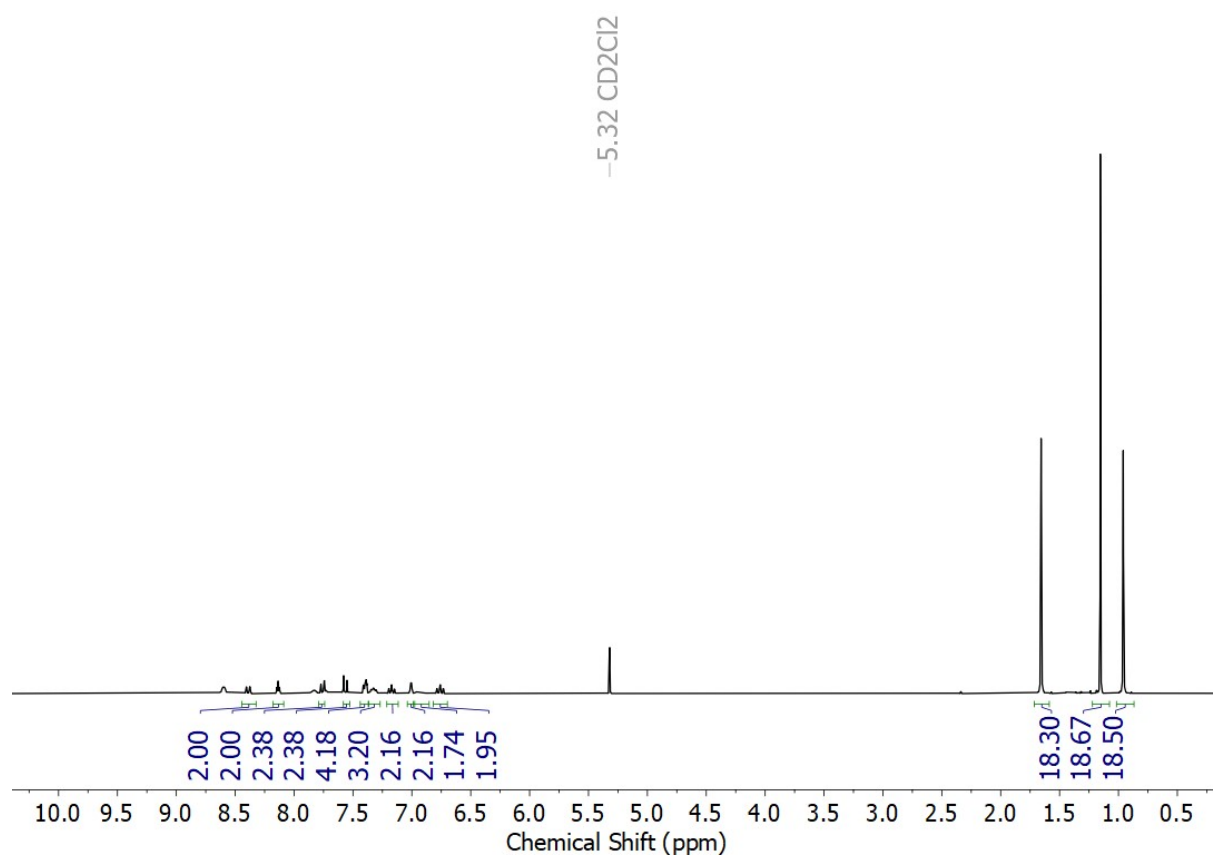### 3.2. Synthesis of [(Mes*P=CH-2-quin)₂Ir(py)]OTf (6)

To a solution of **5** (0.100 g, 0.094 mmol) in dichloromethane (5 mL), 2.5 mL of pyridine was added. The resulting solution was then transferred to a flask containing AgOTf (0.024 g, 0.094 mmol) and was stirred overnight. Subsequently, the reaction mixture was filtered inside the glove box using to remove precipitated AgCl. The filtrate was dried *in vacuo* to obtain pyridine coordinated complex **6** (0.099 g, 0.079 mmol, 84%). X-ray quality crystals were grown at room temperature from a saturated THF solution layered with *n*-hexane (1:5 ratio).

¹H NMR (300 MHz, CD₂Cl₂) δ [ppm] = 0.96 (s, 18H, C(CH_3)₃), 1.15 (s, 18H, C(CH_3)₃), 1.66 (s, 18H, C(CH_3)₃), 6.76 (ddd, J = 8.7, 7.0, 1.6 Hz, 2H, Ar-H), 6.93 (br, 2H, Ar-H), 7.01 (brd, J_{HH} = 1.9 Hz, 2H, Ar-H), 7.17 (t, J_{HH} = 7.4 Hz, 2H, Ar-H), 7.33 (t, J_{HH} = 6.3 Hz, 3H, Ar-H), 7.37 − 7.47 (m, 4H, Ar-H), 7.56 (d, J_{HH} = 8.7 Hz, 2H, Ar-H), 7.76 (d, J_{HH} = 8.7 Hz, 2H, Ar-H), 8.14 (t, J_{PH} = 3.4 Hz, 2H, CH=P), 8.39 (d, J_{HH} = 8.8 Hz, 2H, Ar-H). **³¹P{¹H} NMR** (162 MHz, CD₂Cl₂) δ [ppm] = 244.9. **¹³C{¹H} NMR** (101 MHz, CD₂Cl₂) δ [ppm] = 31.1 (C(CH_3)₃), 33.2 (C(CH_3)₃), 33.9 (C(CH_3)₃), 35.2 (CMe₃), 38.6 (CMe₃), 40.1 (CMe₃), 119.8 (Ar), 120.4 (t, J = 9.4 Hz), 123.4 (Ar), 123.9 (d, J = 11.0 Hz), 124.3 (Ar), 124.6 (Ar), 125.1 (Ar), 125.9 (Ar), 126.9 (Ar), 129.4 (Ar), 129.9 (Ar), 132.1 (t, J = 20.0 Hz), 136.8 (Ar), 137.1 (Ar), 138.5 (Ar), 147.4 (Ar), 150.1 (Ar), 153.4 (Ar), 153.9 (Ar), 154.3 (Ar), 156.2 (Ar), 171.3 (Ar). **IR** (ATR, 32 scans, cm⁻¹): 3066 (w), 2952 (m), 2905 (m), 2866 (m), 2082 (w), 1943 (w), 1845 (w), 1772 (w), 1750 (w), 1717 (w), 1699 (w), 1684 (w), 1653 (w), 1636 (w), 1605 (m), 1548 (m), 1507 (m), 1477 (m), 1447 (m), 1426 (m), 1395 (w), 1347 (s), 1329 (m), 1260 (s), 1221 (s), 1213 (s), 1145 (s), 1121 (s), 1066 (m), 1029 (s), 983 (w), 941 (s), 875 (m), 821 (m), 776 (w), 750 (m), 736 (m), 700 (m), 676 (w), 649 (w), 635 (s), 617 (m), 571 (w), 534 (w), 515 (m), 493 (w), 481 (w), 434 (w). **MS** (ESI-TOF): [M]⁺ expected: m/z = 1106.5216; found: m/z = 1106.5093. **Elemental analysis** for C₆₂H₇₇F₃O₃SN₃P₂Ir: C, 59.31; H, 6.18; N, 3.35 Found: C, 58.06; H, 6.20; N, 3.33.

Figure S4. $^{31}P\{^{1}H\}$ NMR spectrum of **6** (CD$_2$Cl$_2$, 162 MHz, rt).

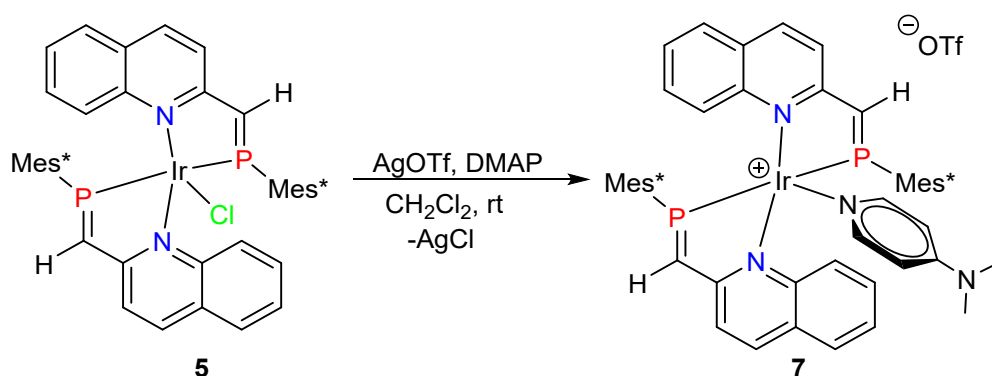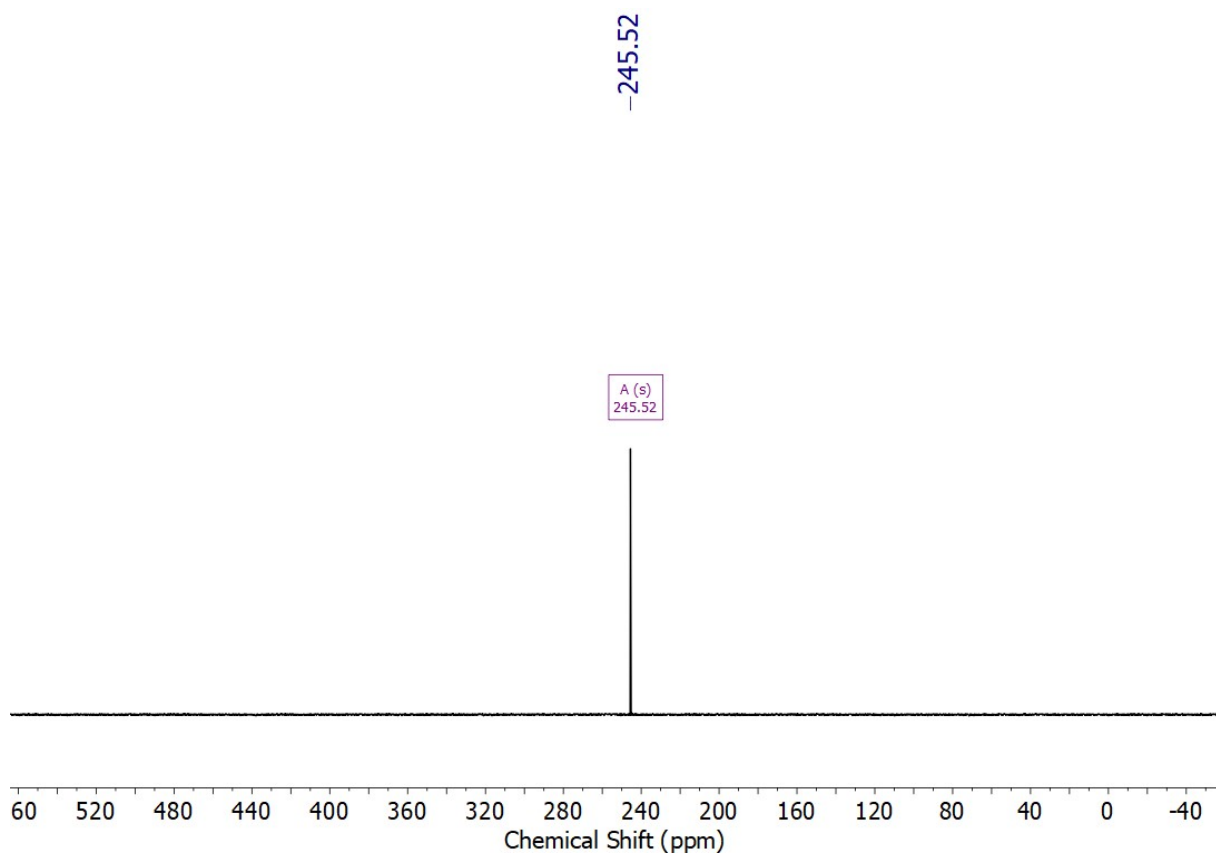**Figure S5.** ^{1}H NMR spectrum of **6** (CD$_2$Cl$_2$, 300 MHz, rt).
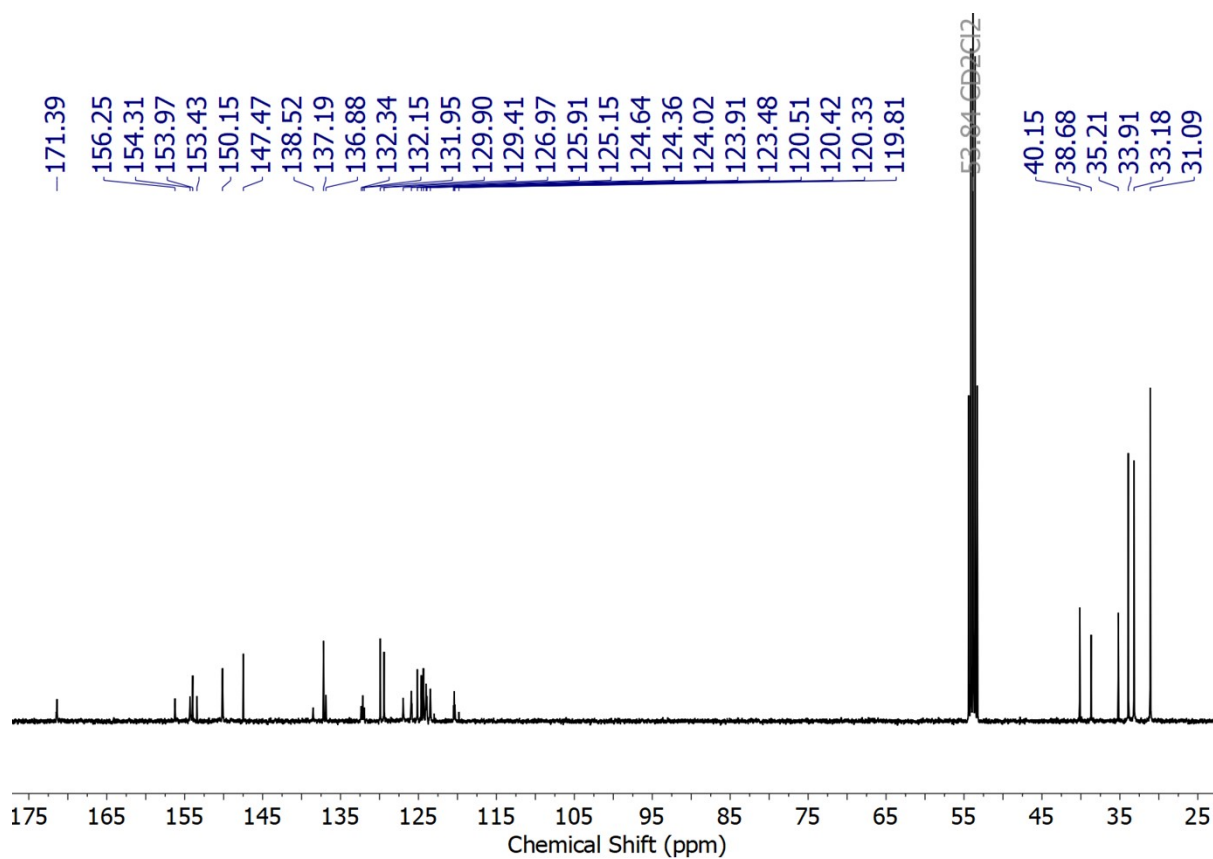
Figure S6. ^{13}C NMR spectrum of **6** (CD$_2$Cl$_2$, 101 MHz, rt).

## 3.3. Synthesis of [(Mes*P=CH-2-quin)₂Ir(dmap)]OTf (7)

Inside a nitrogen filled glove box, complex **5** (0.030 g, 0.028 mmol) and DMAP (0.005 g, 0.040 mmol) were combined and dissolved in dichloromethane (0.6 mL). The resulting reaction mixture was transferred to a vial containing AgOTf (0.007 g, 0.028 mmol) and stirred overnight. Subsequently, the reaction mixture was filtered to remove precipitated AgCl. The filtrate was dried *in vacuo* to obtain complex **7** (0.032 g, 0.024 mmol, 87%).

¹H NMR (400 MHz, CD$_2$Cl$_2$) δ [ppm] = 0.95 (s, 18H, C(CH_3)$_3$), 1.17 (s, 18H, C(CH_3)$_3$), 1.67 (s, 18H, C(CH_3)$_3$), 2.84 (s, 6H, N(CH_3)$_2$), 5.94 – 6.02 (m, 2H, Ar-*H*), 6.82 (ddd, J_{HH} = 8.7, 7.0, 1.6 Hz, 2H, Ar-*H*), 6.96 – 7.04 (m, 2H, Ar-*H*), 7.16 (ddd, J_{HH} = 7.9, 6.9, 1.0 Hz, 2H, Ar-*H*), 7.22 – 7.27 (m, 2H, Ar-*H*), 7.35 (dd, J_{HH} = 7.9, J_{PH} = 1.6 Hz, 2H, Ar-*H*), 7.40 (br, 2H, Ar-*H*), 7.51 (d, J_{HH} = 8.7 Hz, 2H, Ar-*H*), 7.68 (d, J_{HH} = 8.6 Hz, 2H, Ar-*H*), 8.05 (t, J_{PH} = 3.0 Hz, 2H, C*H*=P), 8.48 (d, J_{HH} = 8.8 Hz, 2H, Ar-*H*).
³¹P{¹H} NMR (162 MHz, CD$_2$Cl$_2$) δ [ppm] = 245.5. **¹³C{¹H} NMR** (101 MHz, CD$_2$Cl$_2$) δ [ppm] = 31.1 (C(CH_3)$_3$), 33.2 (C(CH_3)$_3$), 34.1 (C(CH_3)$_3$), 35.2, 38.6, 39.2 (*C*Me$_3$), 39.3 (*C*Me$_3$), 40.2 (*C*Me$_3$), 106.9 (Ar), 108.7 (Ar), 120.2 (Ar), 123.3 (Ar), 123.9 (Ar), 124.4 (Ar), 124.6 (d, J = 8.3 Hz), 126.2 (Ar), 128.5 (Ar), 129.1 (Ar), 129.3 (Ar), 129.9 (Ar), 130.9 (t, J = 19.3 Hz), 136.7 (Ar), 147.8 (Ar), 148.5 (Ar), 152.8 (Ar), 153.4 (Ar), 153.7 (Ar), 153.9 (Ar), 156.1 (Ar), 171.4 (Ar). **IR** (ATR, 32 scans, cm⁻¹): 3066 (w), 2954 (w), 2905 (w), 2868 (w), 1620 (m), 1606 (m), 1537 (w), 1507 (w), 1477 (w), 1444 (w), 1426 (m), 1391 (w), 1347 (s), 1329 (m), 1262 (s), 1223 (s), 1146 (s), 1122 (m), 1061 (w), 1030 (s), 1012 (m), 985 (w), 939 (s), 875 (w), 820 (m), 805 (w), 775 (w), 751 (m), 736 (w), 674 (w), 667 (w), 649 (w), 636 (s), 619 (m), 571 (w), 533 (m), 515 (m), 494 (m), 480 (m), 443 (w), 422 (w). **MS** (ESI-TOF): [M]⁺ expected: m/z = 1149.5638; found: m/z = 1149.5284. **Elemental analysis** for C$_{64}$H$_{82}$F$_3$O$_3$N$_4$P$_2$SIr: C, 59.19; H, 6.36; N, 4.31 Found: C, 58.94; H, 6.01; N, 4.74.

Figure S7. $^{31}P\{^1H\}$ NMR spectrum of **7** (CD$_2$Cl$_2$, 162 MHz, rt).
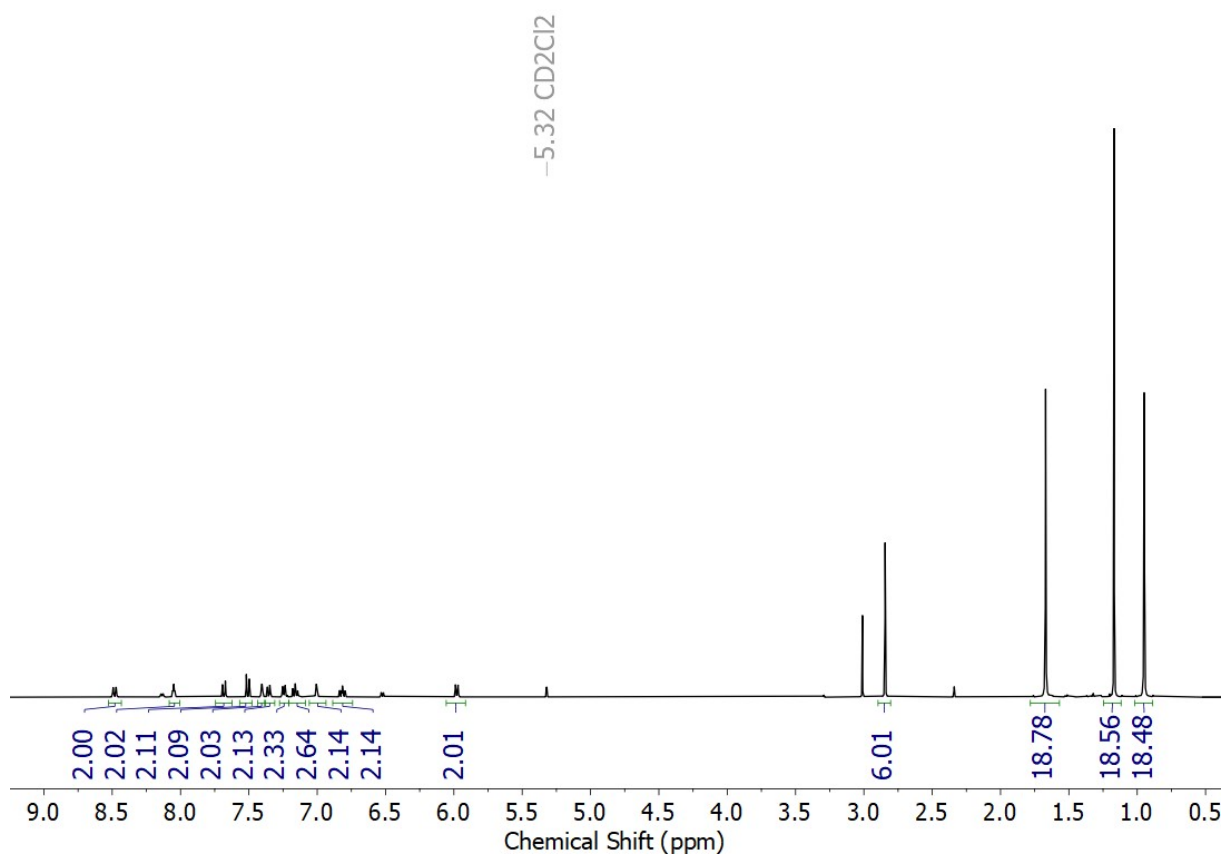
Figure S8. ^1H NMR spectrum of **7** (CD$_2$Cl$_2$, 300 MHz, rt).
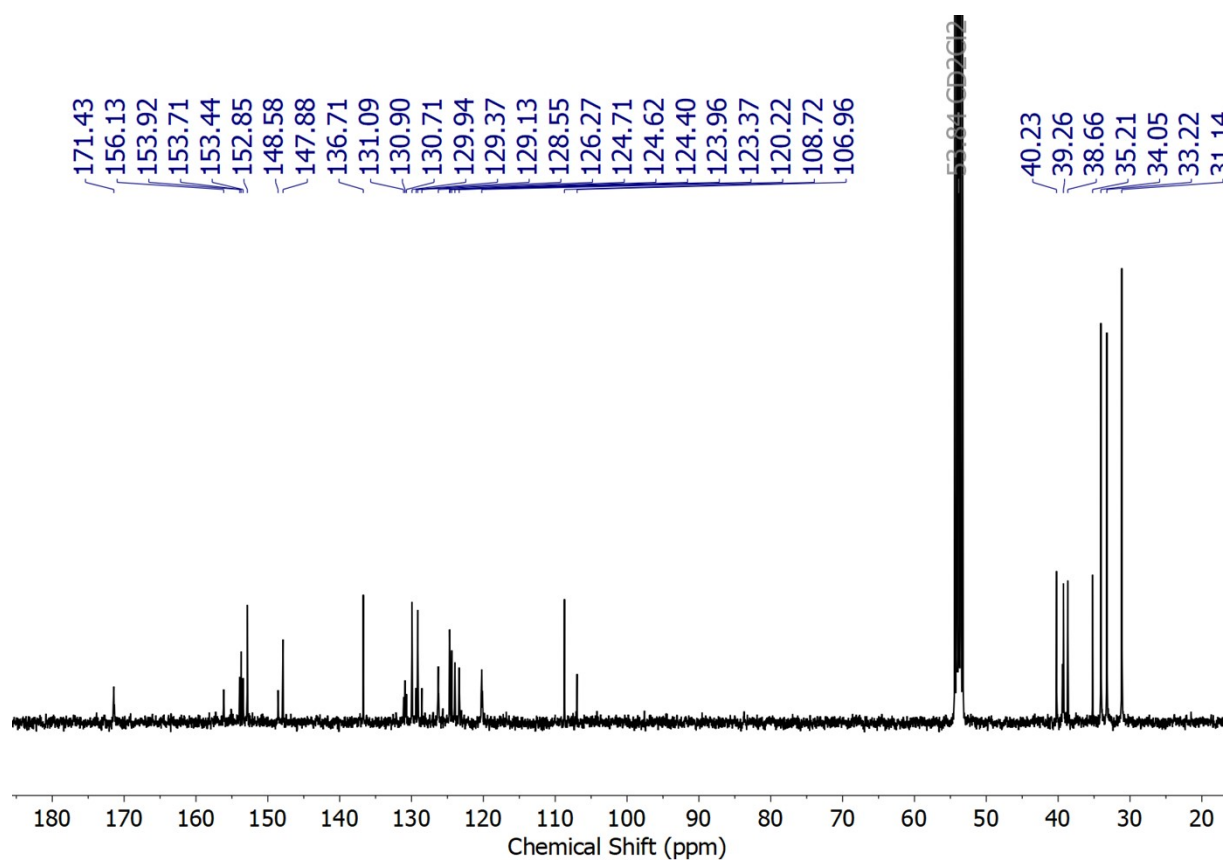
Figure S9. ^{13}C NMR spectrum of **7** (CD$_2$Cl$_2$, 101 MHz, rt)

3.4. Synthesis of Ir(III) hydride complex (8)
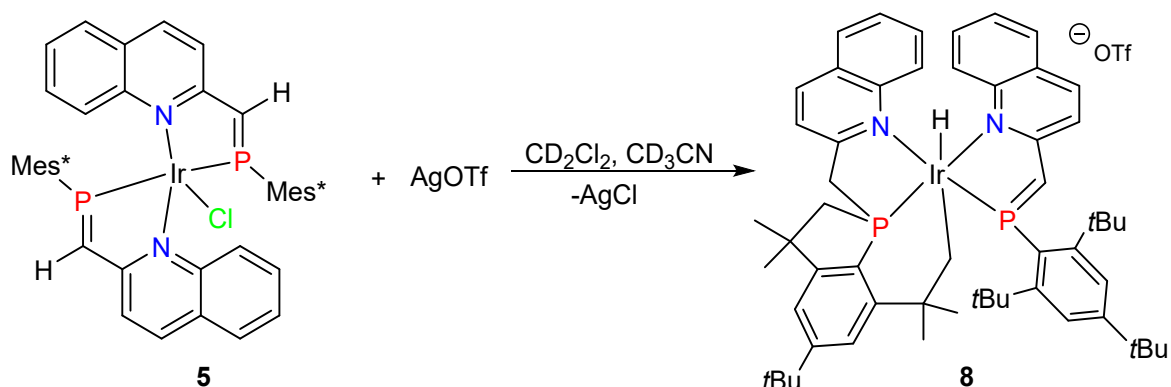
In a 10 mL Schlenk flask, complex **5** (0.096 g, 0.090 mmol) was dissolved in 2:1 ratio of CD_2Cl_2 (0.8 mL) and CD_3CN (0.4 mL). Next AgOTf (0.023 g, 0.090 mmol) was added to the solution. The resulting blue reaction mixture slowly changed to red upon heating at 60 °C for 12 h. Subsequently, the reaction mixture was filtered to remove precipitated AgCl. The filtrate was dried *in vacuo* to obtain a pure solid of Ir (III) hydride complex **8** (0.084 g, 0.071 mmol, 79%). X-ray quality crystals were grown at room temperature from a saturated dichloromethane solution layered with *n*-hexane (1:5 ratio).
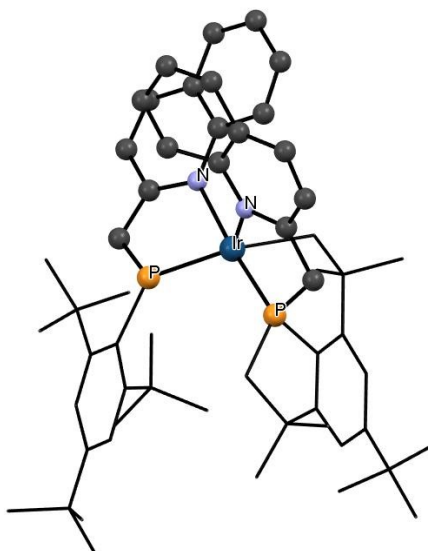
Figure S10. Molecular structure of complex **8** determined by X-ray diffraction analysis. Bond lengths and bond angles are not specified as the data quality was insufficient for a detailed discussion of structural parameters. The Ir−H could not be located in the difference Fourier map. The triflate counterion has been omitted for clarity.

¹H NMR (400 MHz, THF-d$_8$) δ [ppm] = -22.08 (t, J_{PH} = 14.6 Hz, 1H, Ir-*H*), 1.28 (s, 9H, C(C*H$_3$*)$_3$), 1.31-1.35 (m, 15H, C(C*H$_3$*)$_3$, C-(C*H$_3$*)$_2$), 1.37 (s, 9H, C(C*H$_3$*)$_3$), 1.38 (s, 9H, C(C*H$_3$*)$_3$), 1.53 (br, 3H, C-(C*H$_3$*)$_2$), 1.57 (br, 3H, C-(C*H$_3$*)$_2$), 1.97 (dd, J_{HH} = 15.2, J_{PH} = 7.7 Hz, 1H, C*H$_2$*), 2.59 (dd, J_{HH} = 15.2, J_{PH} = 6.1 Hz, 1H, C*H$_2$*), 2.73 – 2.83 (m, 2H, CH$_2$), 4.66 (dd, J_{HH} = 19.2, J_{PH} = 10.9 Hz, 1H, C*H$_2$*), 5.00 (dd, J_{HH} = 19.2, J_{PH} = 10.4 Hz, 1H, C*H$_2$*), 6.84 (ddd, J_{HH} = 8.6, 6.9, 1.5 Hz, 1H, Ar-*H*), 7.02 (ddd, J_{HH} = 8.8, 7.0, 1.6 Hz, 1H, Ar-*H*), 7.17 – 7.24 (m, 2H, Ar-*H*), 7.28 (ddd, J_{HH} = 8.0, 6.9, 1.1 Hz, 1H, Ar-*H*), 7.35 (ddd, J_{HH} = 7.9, 6.9, 1.0 Hz, 1H, Ar-*H*), 7.44 (dd, J_{HH} = 4.7, J_{PH} = 1.6 Hz, 1H, Ar-*H*), 7.50 (dd, J_{HH} = 8.8, J_{PH} = 1.0 Hz, 1H, Ar-*H*), 7.56 (br, 1H, Ar-*H*), 7.74 (br, 1H, Ar-*H*), 7.89 (dt, J_{HH} = 8.2, J_{PH} = 1.4 Hz, 2H, Ar-*H*), 7.94 (dd, J_{HH} = 8.1, $J_{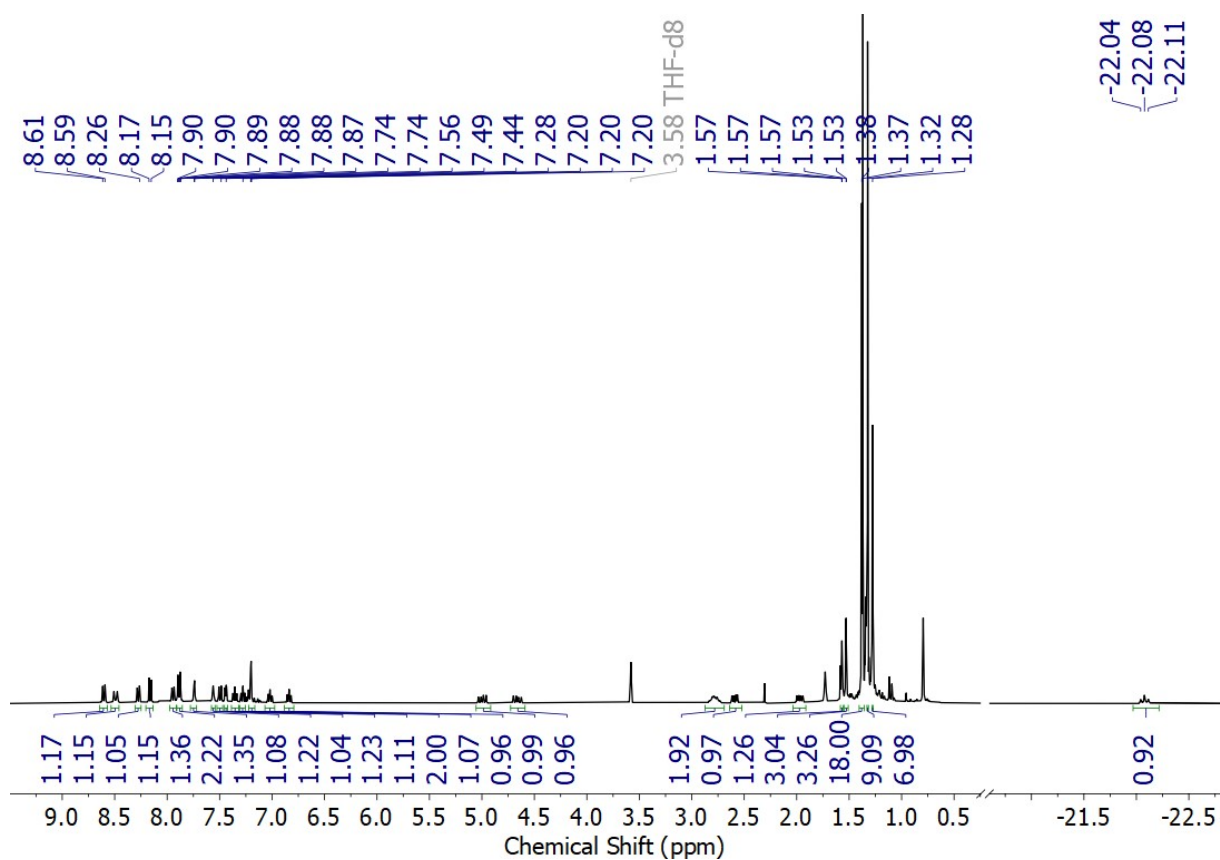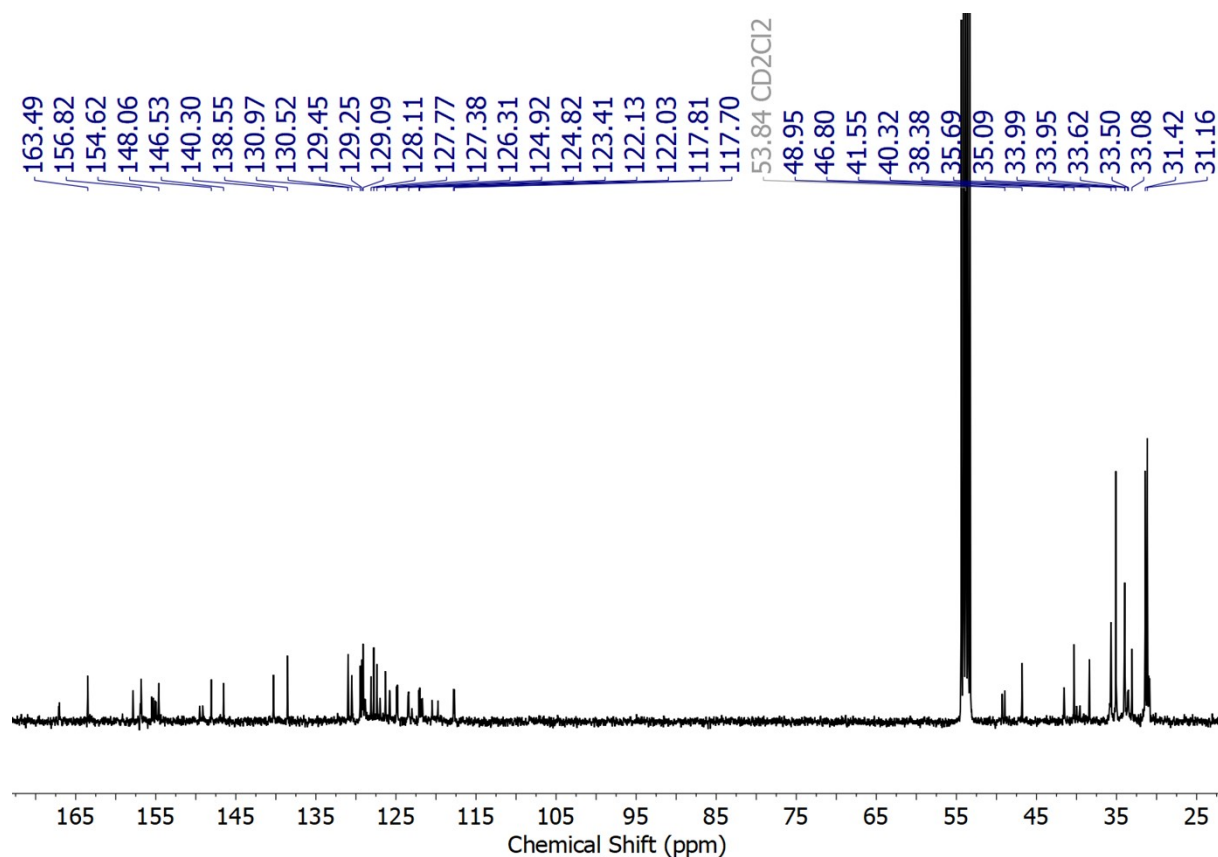PH}$ = 1.5 Hz, 1H, Ar-*H*), 8.16 (d, J_{HH} = 8.5 Hz, 1H, Ar-*H*), 8.27 (d, J_{HH} = 8.6 Hz, 1H, Ar-*H*), 8.49 (d, J = 13.0 Hz, 1H), 8.60 (dt, J_{HH} = 8.5, J_{PH} = 1.0 Hz, 1H, Ar-*H*). **³¹P{¹H} NMR** (162 MHz, THF-d$_8$) δ [ppm] = 285.5 (t, J = 11.6 Hz), 6.8 (t, J = 11.0 Hz). **¹³C{¹H} NMR** (101 MHz, THF-d8) δ [ppm] = 31.1, 31.4, 33.1, 33.5 (d, J = 11.7 Hz), 33.9 (d, J = 3.1 Hz), 35.1, 35.6, 38.3, 39.7 (d, J = 42.0 Hz), 40.3, 41.5, 46.8, 48.9, 49.2, 117.7 (d, J = 11.1 Hz), 119.7 (Ar), 120.4 (Ar), 121.7 (d, J = 17.2 Hz), 122.0 (d, J = 10.2 Hz), 123.4 (Ar), 124.8 (d, J = 10.1 Hz), 125.7 (Ar), 126.3 (Ar), 126.9 (Ar), 127.3 (Ar), 127.7 (Ar), 128.1 (Ar), 128.9 (Ar), 129.1 (Ar), 129.2 (Ar), 129.4 (Ar), 130.5 (Ar), 130.9 (Ar), 138.5 (Ar), 140.3 (Ar), 146.5 (Ar), 148.1 (Ar), 149.3 (d, J = 39.1 Hz), 154.6 (Ar), 155.0 (d, J = 12.1 Hz), 155.4 (d, J = 19.3 Hz), 156.8 (Ar), 157.8 (Ar), 163.4 (Ar), 167.0 (Ar). **IR** (ATR, 32 scans, cm^{-1}): 3477 (w), 3064 (w), 2956 (m), 2868 (m), 2349 (w), 1597 (m), 1546 (w), 1509 (m), 1462 (w), 1428 (w), 1395 (w), 1361 (m), 1322 (w), 1258 (s), 1222 (m), 1148 (s), 1123 (m), 1076 (w), 1029 (s), 981 (w), 958 (w), 914 (w), 875 (m), 840 (m), 752 (m), 711 (w), 684 (w), 666 (w), 636 (s), 572 (w), 556 (w), 516 (m), 497 (w), 473 (w), 458 (w), 425 (w). **MS** (ESI-TOF): [M]$^+$ expected: m/z = 1027.4800; found: m/z = 1027.4800.

−285.09

−6.91

A (s)
285.09

B (s)
6.91

550 500 450 400 350 300 250 200 150 100 50 0 -50 -100 -150 -200 -250
Chemical Shift (ppm)
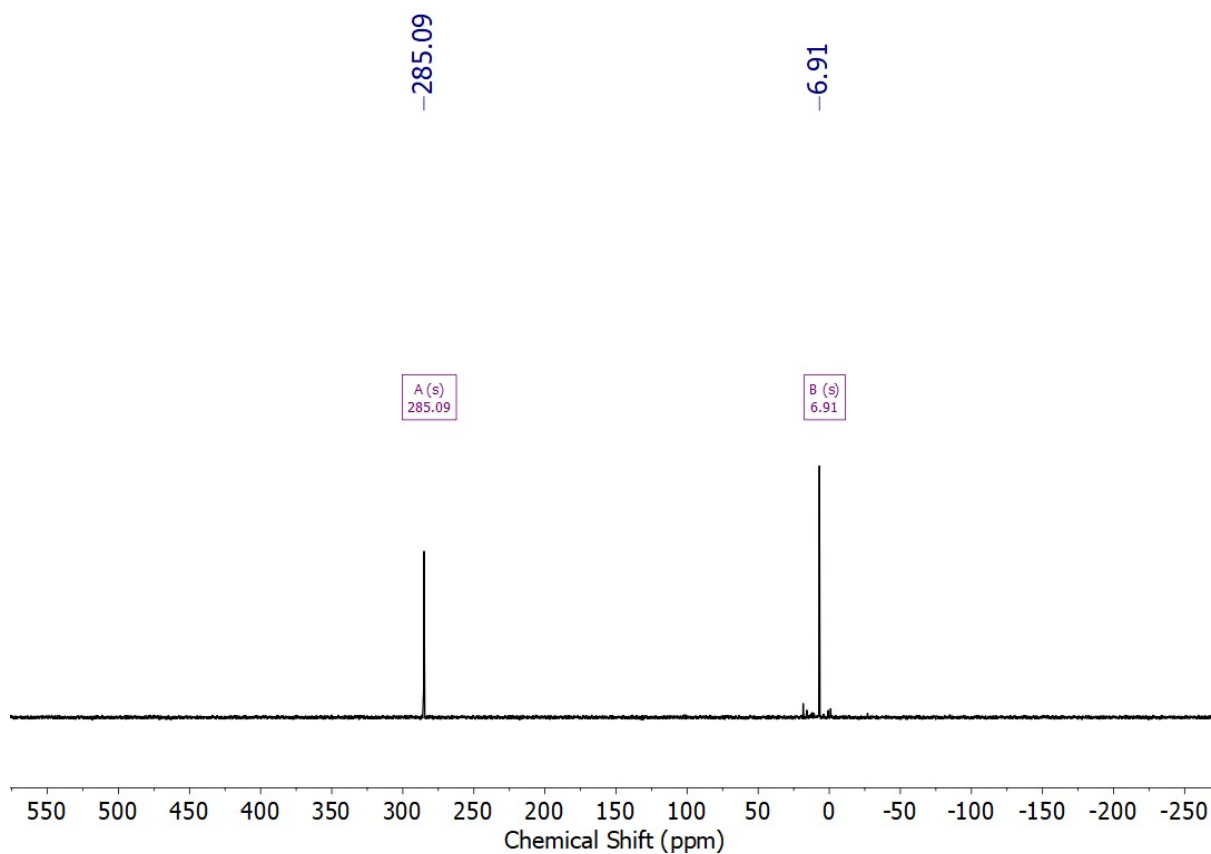
Figure S11. ^{31}P{^{1}H} NMR spectrum of **8** (thf-d$_8$, 162 MHz, rt).

3.58 THF-d8

−22.04
−22.08
−22.11

8.61
8.59
8.26
8.17
8.15
7.90
7.90
7.89
7.88
7.88
7.87
7.74
7.74
7.56
7.49
7.44
7.28
7.20
7.20
7.20

1.57
1.57
1.57
1.53
1.53
1.38
1.37
1.32
1.28

1.17
1.15
1.05
1.15
1.36
2.22
1.35
1.08
1.22
1.04
1.23
1.11
2.00
1.07
0.96
0.99
0.96

1.92
0.97
1.26
3.04
3.26
18.00
9.09
6.98

0.92

9.0 8.5 8.0 7.5 7.0 6.5 6.0 5.5 5.0 4.5 4.0 3.5 3.0 2.5 2.0 1.5 1.0 0.5 -21.5 -22.5
Chemical Shift (ppm)

Figure S12. ^{1}H NMR spectrum of **8** (thf-d$_8$, 400 MHz, rt).

Figure S13. ^{13}C NMR spectrum of **8** (CD$_2$Cl$_2$, 101 MHz, rt).

3.5. Synthesis of [(Mes*P=CH-2-quin)$_2$Ir(CO)]BF$_4$ (9)
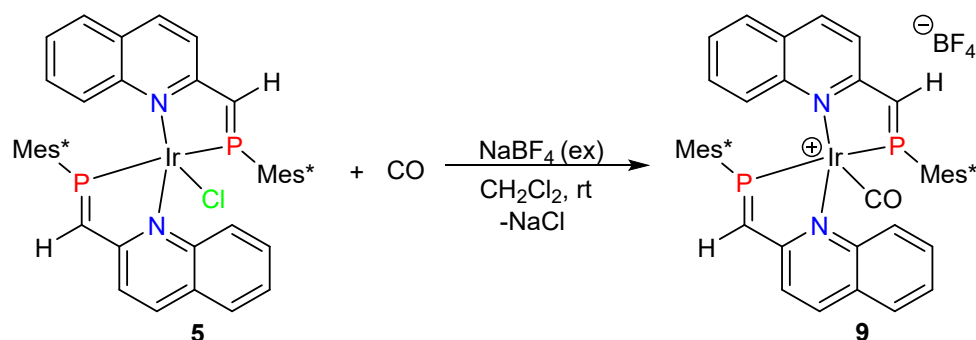
To a solution of **5** (0.050 g, 0.047 mmol) in dichloromethane (20 mL), an excess of NaBF$_4$ (0.024 g, 0.218 mmol) was added. The dark blue solution was stirred for 4 h under a constant flow of freshly generated CO gas (1 atm). The colour of the solution slowly changed from dark blue to turquoise. Subsequently, the reaction mixture was filtered to remove precipitated NaCl and remaining NaBF$_4$. The resulting turquoise solution was dried *in vacuo* to obtain complex **9** (0.048 g, 0.042 mmol, 89%). X-ray quality crystals were grown at room temperature from a saturated 1,2-diflourobenzene solution layered with *n*-hexane (1:5 ratio).

¹H NMR (400 MHz, CD$_2$Cl$_2$) δ [ppm] = 0.93 (s, 18H, C(CH_3)), 1.21 (s, 18H, C(CH_3)), 1.75 (s, 18H, C(CH_3)), 7.02 (brd, J_{HH} = 1.9 Hz, 2H, Ar-H), 7.32 – 7.46 (m, 4H, Ar-H), 7.58 (brd, J_{HH} = 1.6 Hz, 2H, Ar-H), 7.63 (dd, J_{HH} = 7.8, J_{PH} = 1.8 Hz, 2H), 7.78 (d, J_{HH} = 8.6 Hz, 2H), 8.03 (d, J_{HH} = 8.6 Hz, 2H), 8.32 (t, J_{PH} = 5.4 Hz, 2H, CH=P), 8.96 (d, J_{HH} = 8.6 Hz, 2H, Ar-H). **³¹P{¹H} NMR** (162 MHz, CD$_2$Cl$_2$) δ [ppm] = 271.4. **¹³C{¹H} NMR** (101 MHz, CD$_2$Cl$_2$) δ [ppm] = 31.0 (C(CH_3)$_3$), 32.9 (C(CH_3)$_3$), 34.1 (C(CH_3)$_3$), 35.4 (CMe$_3$), 38.4 (CMe$_3$), 40.6 (CMe$_3$), 121.9 (Ar), 125.2 (Ar), 125.5 (Ar), 127.3 (Ar), 128.5 (Ar), 129.4 (Ar), 131.0 (Ar), 138.1 (Ar), 148.7 (Ar), 154.7 (Ar), 155.4 (Ar), 168.9, 174.3 (Ar). **IR** (ATR, 32 scans, cm^{-1}): 3072 (m), 2955 (m), 2906 (m), 2868 (m), 2367 (w), 2236 (w), 2091 (w), 2051 (w), 1978 (s), 1604 (m), 1550 (m), 1508 (m), 1467 (m), 1445 (m), 1428 (m), 1396 (m), 1360 (s), 1329 (m), 1281 (w), 1237 (m), 1212 (m), 1178 (w), 1148 (m), 1122 (m), 1051 (s), 991 (m), 957 (s), 933 (m), 903 (w), 875 (m), 831 (m), 777 (w), 748 (m), 734 (m), 708 (w), 676 (w), 650 (w), 639 (w), 619 (m), 581 (w), 534 (w), 517 (w), 498 (w), 477 (w), 460 (w). **MS** (ESI-TOF): [M-CO]$^+$expected: m/z = 1027.4794; found: m/z = 1027.4834. **Elemental analysis** for C$_{57}$H$_{72}$BF$_4$ON$_2$P$_2$Ir: C, 59.94; H, 6.35; N, 2.45 Found: C, 59.08; H, 6.55; N, 2.20.
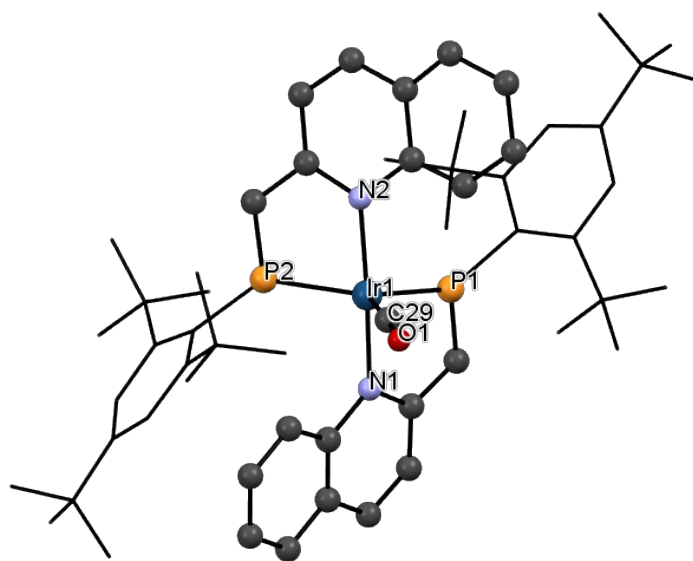
Figure S14. Molecular structure of complex **9** determined by X-ray diffraction analysis. Bond lengths and bond angles are not specified as the data quality was insufficient for a detailed discussion of structural parameters.
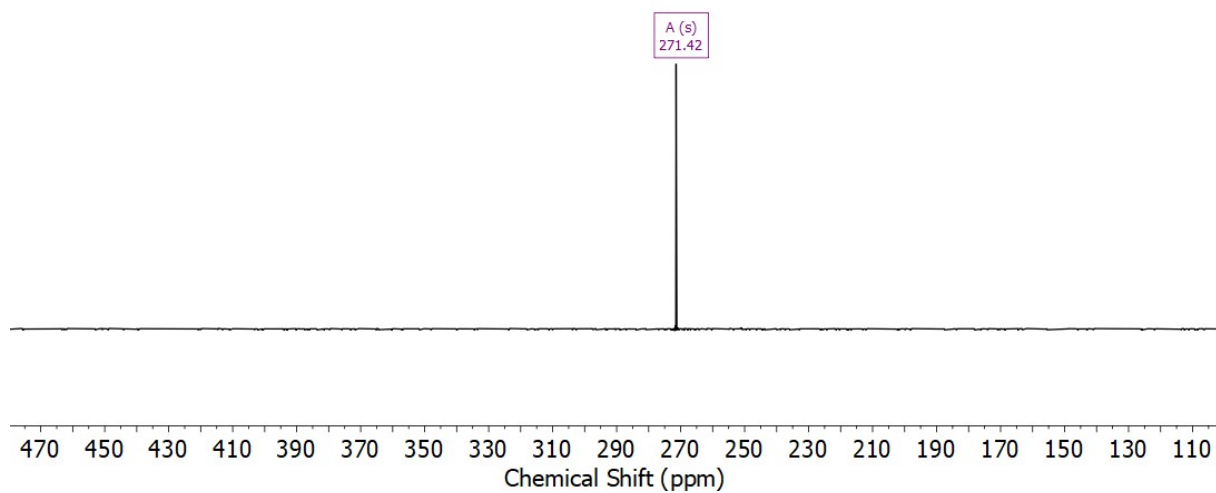
Figure S15. $^{31}P\{^1H\}$ NMR spectrum of **9** (CD$_2$Cl$_2$, 122 MHz, rt).
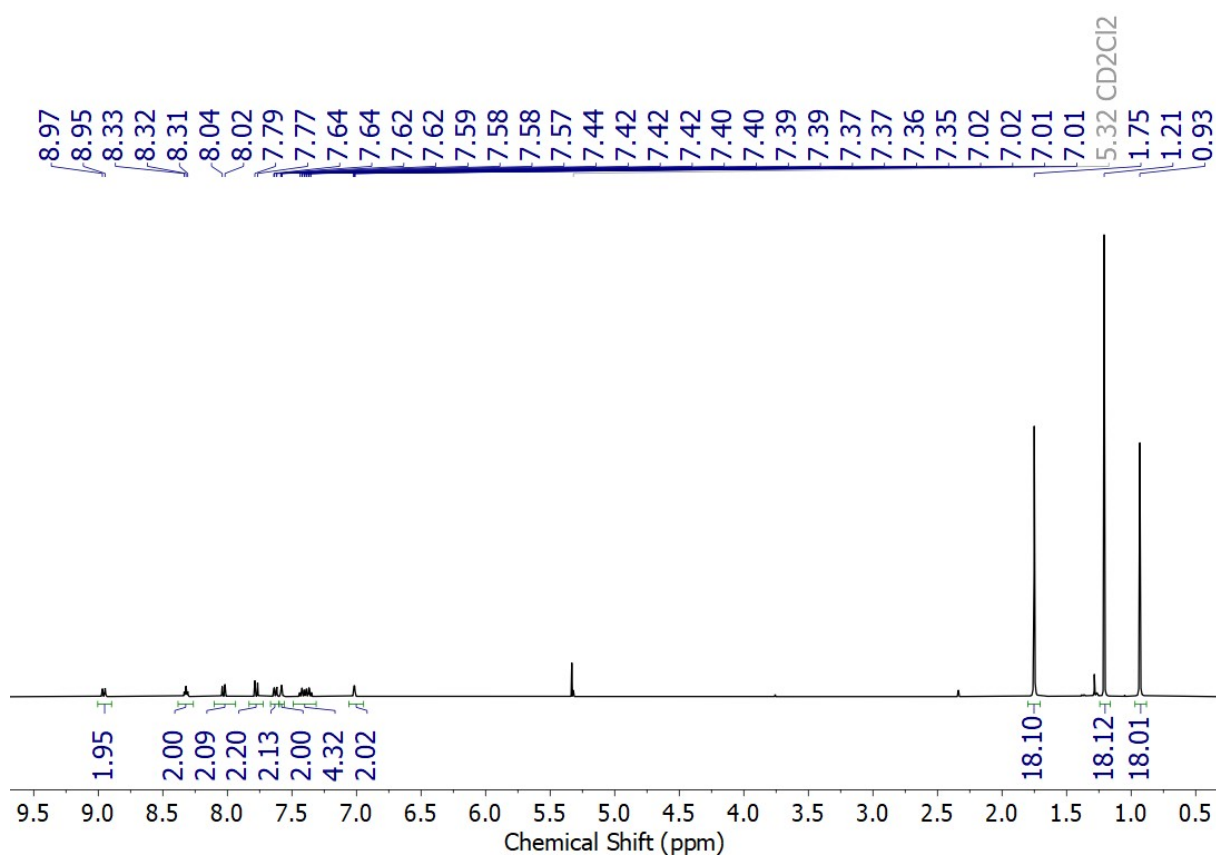
Figure S16. ^1H NMR spectrum of **9** (CD$_2$Cl$_2$, 300 MHz, rt).
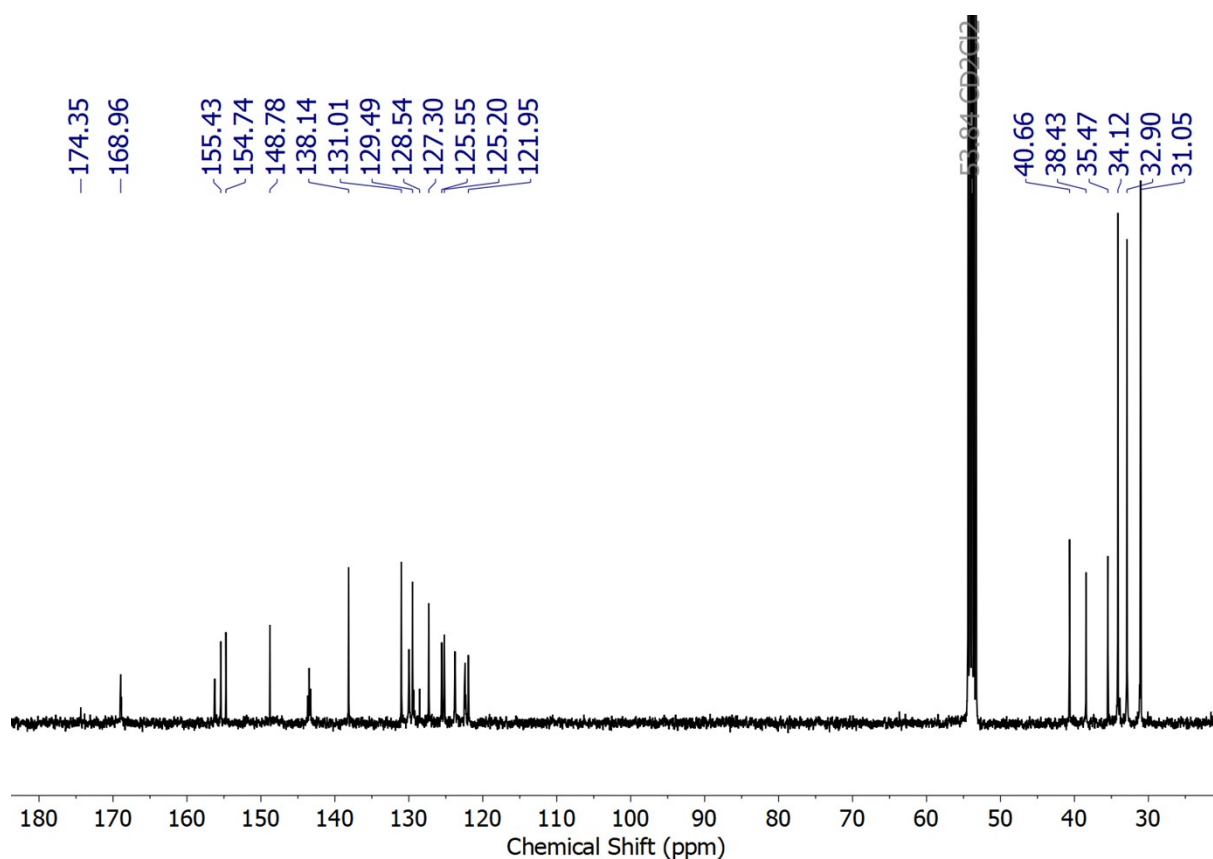
Figure S17. ^{13}C NMR spectrum of **9** (CD$_2$Cl$_2$, 101 MHz, rt)

3.6. Synthesis of [(Mes*P=CH-2-quin)$_2$Ir(CH$_3$)](10)
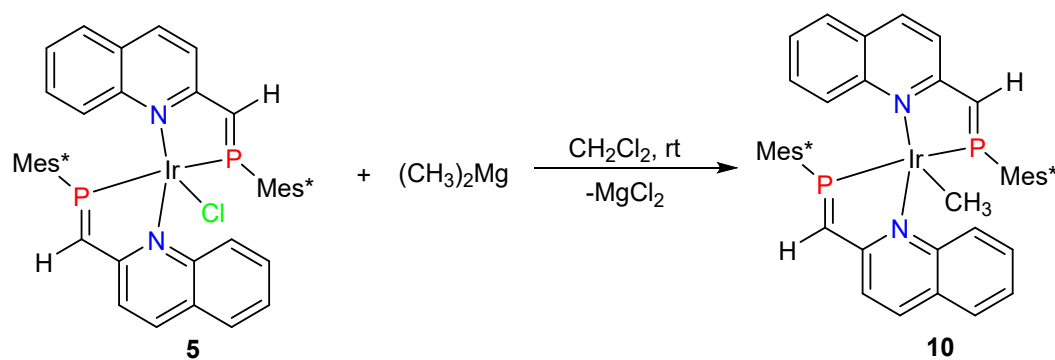
In a 10 mL Schlenk flask, complex **5** (0.200 g, 0.188 mmol) and (CH$_3$)$_2$Mg (0.061 g, 1.129 mmol) were dissolved in 6 mL CH$_2$Cl$_2$ inside the glove box. The reaction mixture turned into a dark turquoise solution and was stirred for 30 minutes. Subsequently, the reaction mixture was filtered to remove precipitated MgCl$_2$. The resulting clear dark solution was concentrated and stored at 0 °C to obtain x-ray quality crystals of complex **10** (0.134 g, 0.128 mmol, 68%).

¹H NMR (300 MHz, CD$_2$Cl$_2$) δ [ppm] = 0.91 (s, 3H, CH_3), 0.95 (s, 18H, C(CH_3)), 1.21 (s, 18H, C(CH_3)), 1.68 (s, 18H, C(CH_3)), 6.83 (ddd, J = 8.7, 6.9, 1.7 Hz, 2H, Ar-H), 6.95 – 7.06 (m, 4H, Ar-H), 7.16 (dd, J = 7.7, 1.7 Hz, 2H, Ar-H), 7.22 (d, J_{HH} = 8.8 Hz, 2H, Ar-H), 7.32 (d, J_{HH} = 8.8 Hz, 2H,

Ar-*H*), 7.56 (br, 2H, Ar-*H*), 7.69 (vt, J_{app} = 1.5 Hz, 2H, C*H*=P), 8.71 (d, J_{HH} = 8.8 Hz, 2H, Ar-*H*).

^{31}P{^{1}H} NMR (122 MHz, CD_2Cl_2) δ [ppm] = 250.0. **^{13}C{^{1}H} NMR** (101 MHz, THF-d8) δ [ppm] = 31.7 (C(*CH$_3$*)$_3$), 34.0 (*CH$_3$*), 34.1 (br, C(*CH$_3$*)$_3$), 35.6 (*C*Me$_3$), 39.1 (*C*Me$_3$), 40.6 (*C*Me$_3$), 121.1 (Ar), 122.6 (Ar), 123.2 (Ar), 124.5 (br, P=C), 124.8 (Ar), 128.2 (Ar), 129.3 (d, J_{PC} = 8.1 Hz, Ar), 132.3 (Ar), 150.1 (Ar), 152.5 (Ar), 156.1 (Ar), 169.8 (Ar). **IR (ATR, 32 scans, cm-1)**: 3048 (w), 2949 (m), 2904 (m), 2866 (w), 1611 (m), 1594 (w), 1548 (w), 1503 (w), 1478 (w), 1444 (w), 1423 (m), 1392 (w), 1355 (s), 1340 (s), 1269 (w), 1238 (w), 1210 (w), 1176 (w), 1147 (w), 1137 (w), 1122 (w), 1041 (w), 978 (w), 945 (w), 919 (s), 872 (w), 811 (s), 748 (s), 737 (m), 690 (w), 665 (w), 647 (w), 636 (w), 618 (m), 580 (w), 533 (w), 514 (w), 496 (w). **MS** (ESI-TOF): expected: m/z = 1041.5089; found: m/z = 1041.5093. **Elemental analysis** for $C_{57}H_{75}N_2P_2Ir$: C, 65.68; H, 7.25; N, 2.69 Found: C, 65.53; H, 7.57; N, 2.43.
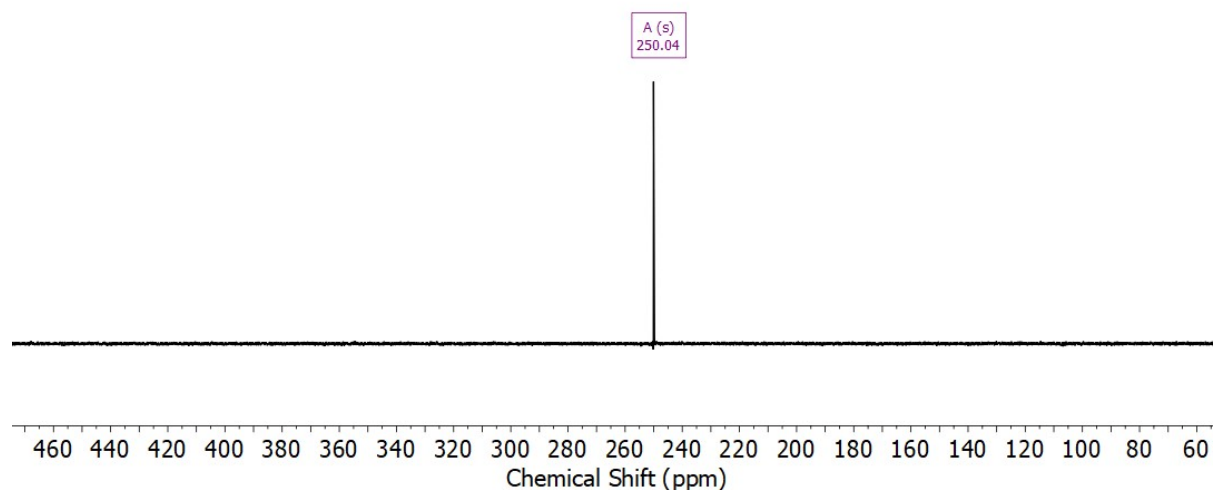
Figure S18. ^{31}P{^{1}H} NMR spectrum of **10** (CD_2Cl_2, 122 MHz, rt).
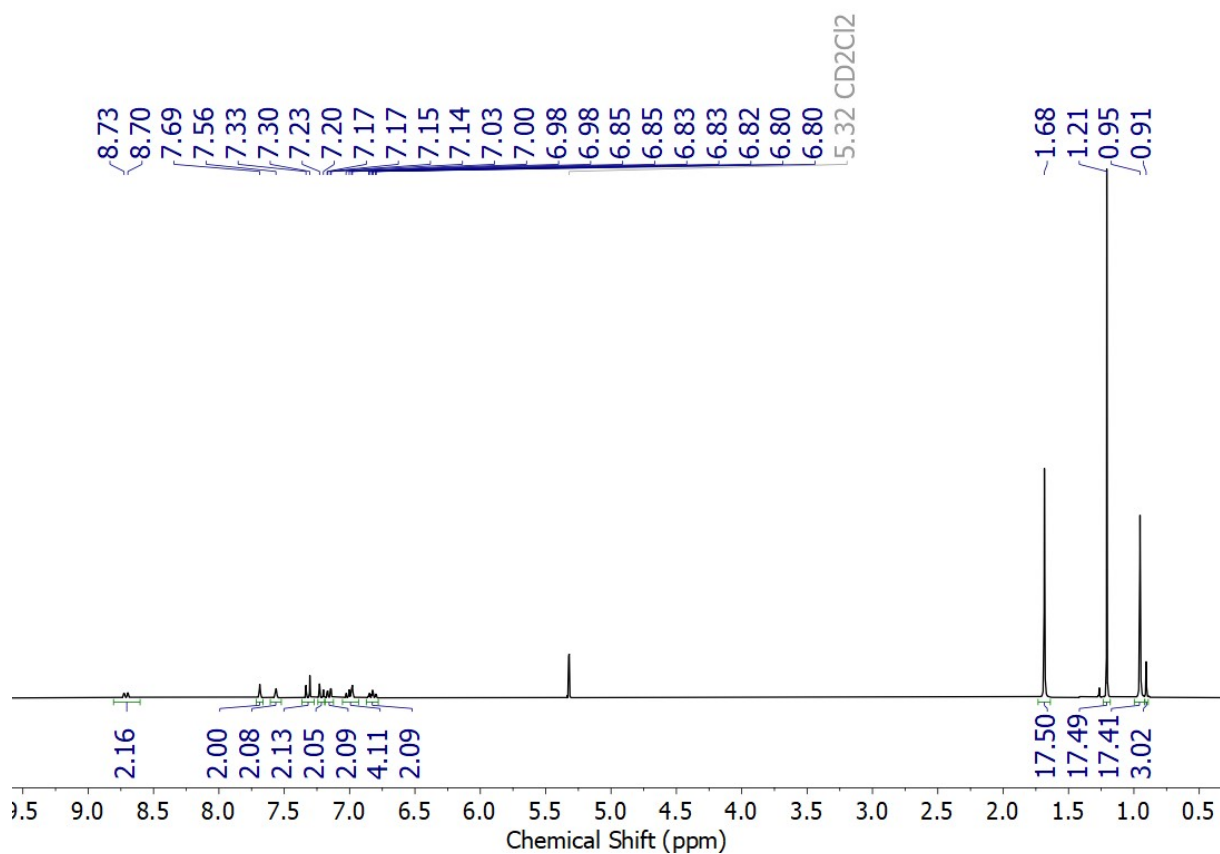
Figure S19. ^{1}H NMR spectrum of **10** (CD$_2$Cl$_2$, 300 MHz, rt).
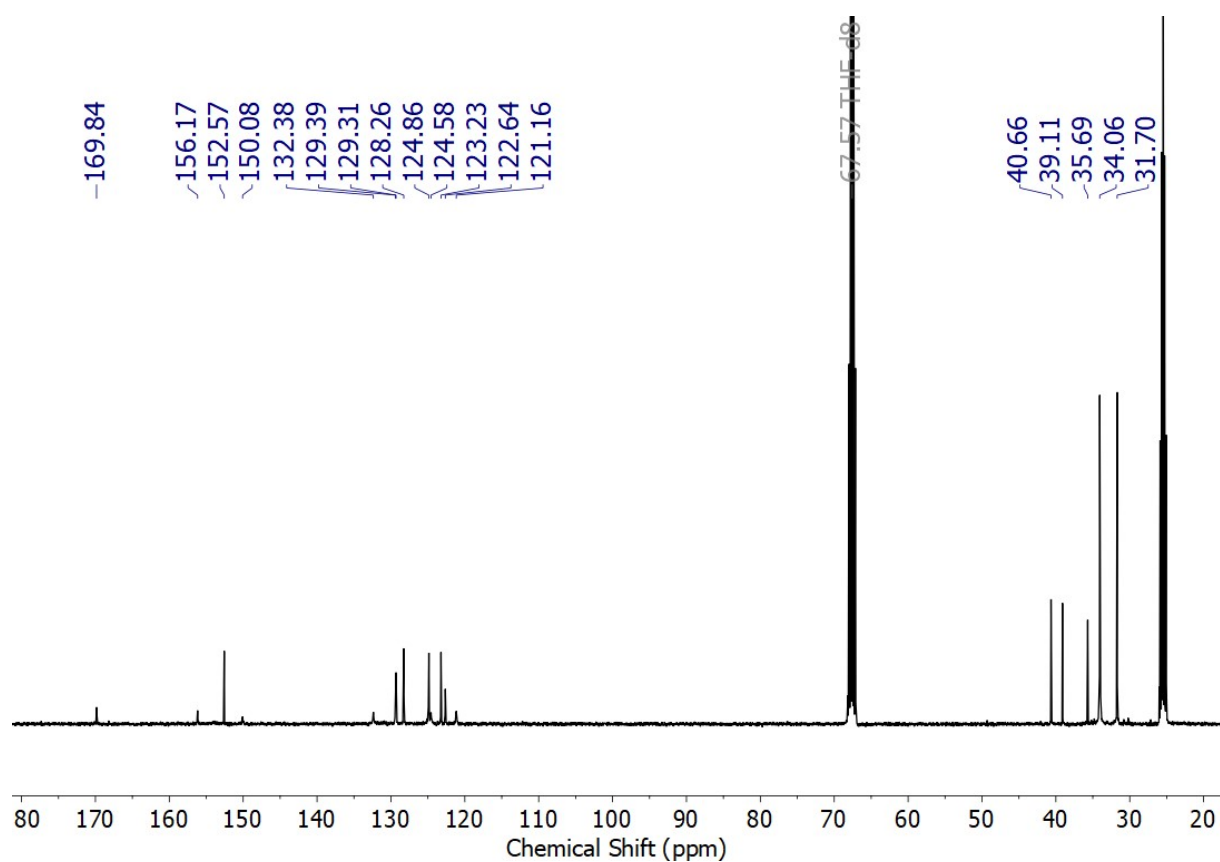
Figure S20. ^{13}C{^{1}H} NMR spectrum of **10** (THF-d8, 101 MHz, rt).

3.7. Synthesis of [(quin-CH=PMes*)₂Ir(N₃)] (11)
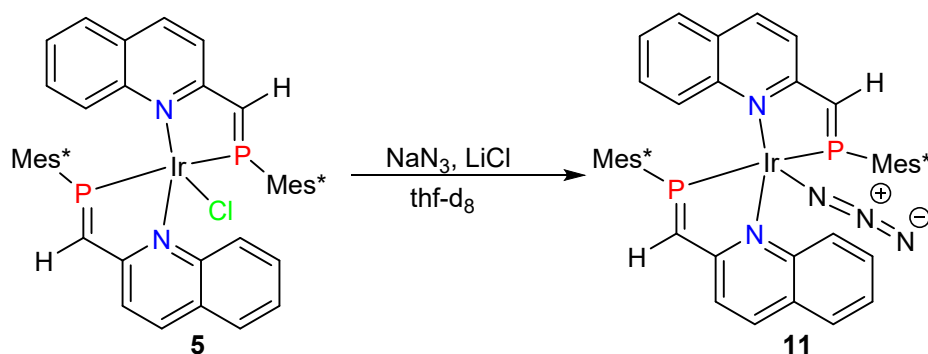
Compound **5** (0.050 g, 0.047 mmol), NaN₃ (0.015 g, 0.234 mmol) and LiCl (0.010 g, 0.234 mmol) were combined in a 5 mL Schlenk tube and dissolved in thf (2 mL). The reaction mixture was stirred vigorously for 8 days at room temperature. The resulting dark green solution was filtered inside the glove box and the filtrate was dried *in vacuo* to obtain iridium azide complex **11** (0.040 mg, 0.037 mmol, 79%) as analytically pure solid. X-ray quality crystals were grown at room temperature from a saturated THF solution layered with *n*-hexane (1:5 ratio).
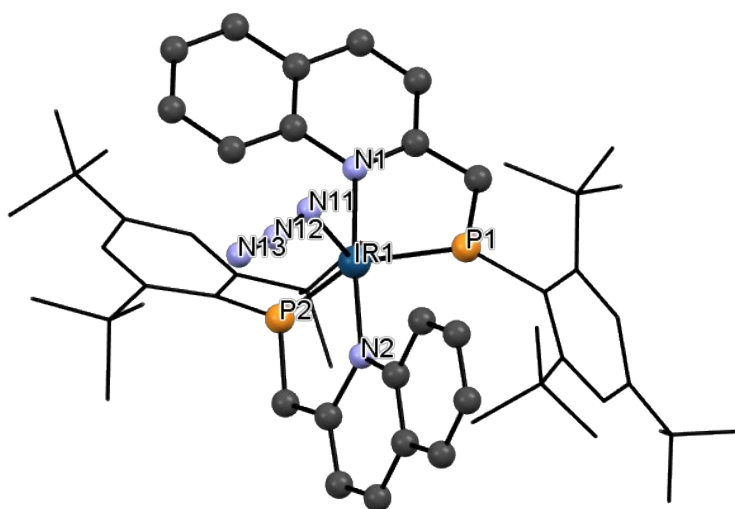
Figure S21. Molecular structure of complex **11** determined by X-ray diffraction analysis. Bond lengths and bond angles are not specified as the data quality was insufficient for a detailed discussion of structural parameters.

¹H NMR (400 MHz, THF-d₈) δ [ppm] = 1H NMR (400 MHz, THF) δ 0.97 (s, 1H), 1.21 (s, 1H), 1.73 (s, 1H), 7.01 (s, 0H), 7.14 (pd, J = 6.9, 1.7 Hz, 0H), 7.24 (dd, J = 7.3, 2.1 Hz, 0H), 7.38 (d, J = 8.7 Hz, 0H), 7.48 (d, J = 8.6 Hz, 0H), 7.86 (d, J = 2.3 Hz, 0H), 9.52 (d, J = 7.7 Hz, 0H). 0.97 (s, 18H, C(CH₃)₃), 1.21 (s, 18H, C(CH₃)₃), 1.73 (s, 18H, C(CH₃)₃), 7.01 (br, 2H, Ar-H), 7.09 – 7.20 (m, 4H, Ar-

H), 7.24 (dd, J_{HH} = 7.3, J_{PH} = 2.1 Hz, 2H, Ar-*H*), 7.38 (d, J_{HH} = 8.7 Hz, 2H, Ar-*H*), 7.48 (d, J_{HH} = 8.6 Hz, 4H, Ar-*H*), 7.86 (t, J_{PH} = 2.3 Hz, 2H, C*H*=P), 9.52 (d, J_{HH} = 7.7 Hz, 2H, Ar-*H*). **^{31}P{^{1}H} NMR** (162 MHz, THF-d_8) δ [ppm] = 243.0. **^{13}C{^{1}H} NMR** (101 MHz, THF-d_8) δ [ppm] = 31.6 (C(*CH*$_3$)$_3$), 33.6 (C(*CH*$_3$)$_3$), 34.3 (C(*CH*$_3$)$_3$), 35.6 (*C*Me$_3$), 39.0 (*C*Me$_3$), 40.9 (*C*Me$_3$), 119.9 (Ar), 123.1 (Ar), 124.2 (Ar), 124.4 (Ar), 124.5 (Ar), 128.1 (Ar), 128.3 (Ar), 128.6 (Ar), 130.3 (Ar), 135.9 (Ar), 150.4 (Ar), 153.1 (Ar), 154.9 (Ar), 155.8 (Ar), 171.5 (Ar). **IR** (ATR, 32 scans, cm^{-1}): 2955 (m), 2902 (w), 2867 (w), 2173 (w), 2059 (w), 2020 (s), 1606 (m), 1549 (w), 1505 (w), 1478 (w), 1465 (w), 1445 (w), 1425 (m), 1392 (w), 1345 (s), 1329 (m), 1284 (w), 1252 (w), 1238 (w), 1211 (w), 1176 (w), 1148 (w), 1122 (w), 1026 (w), 983 (w), 933 (s), 874 (w), 818 (s), 773 (w), 750 (m), 737 (m), 710 (w), 691 (w), 671 (w), 618 (m), 534 (w), 522 (w), 512 (w), 494 (m), 480 (m). **MS** (ESI-TOF): [M-N$_3$]$^+$ expected: m/z = 1027.4781; found: m/z = 1025.4795. Due to the thermal instability elemental analytical data of **11** were not attempted.
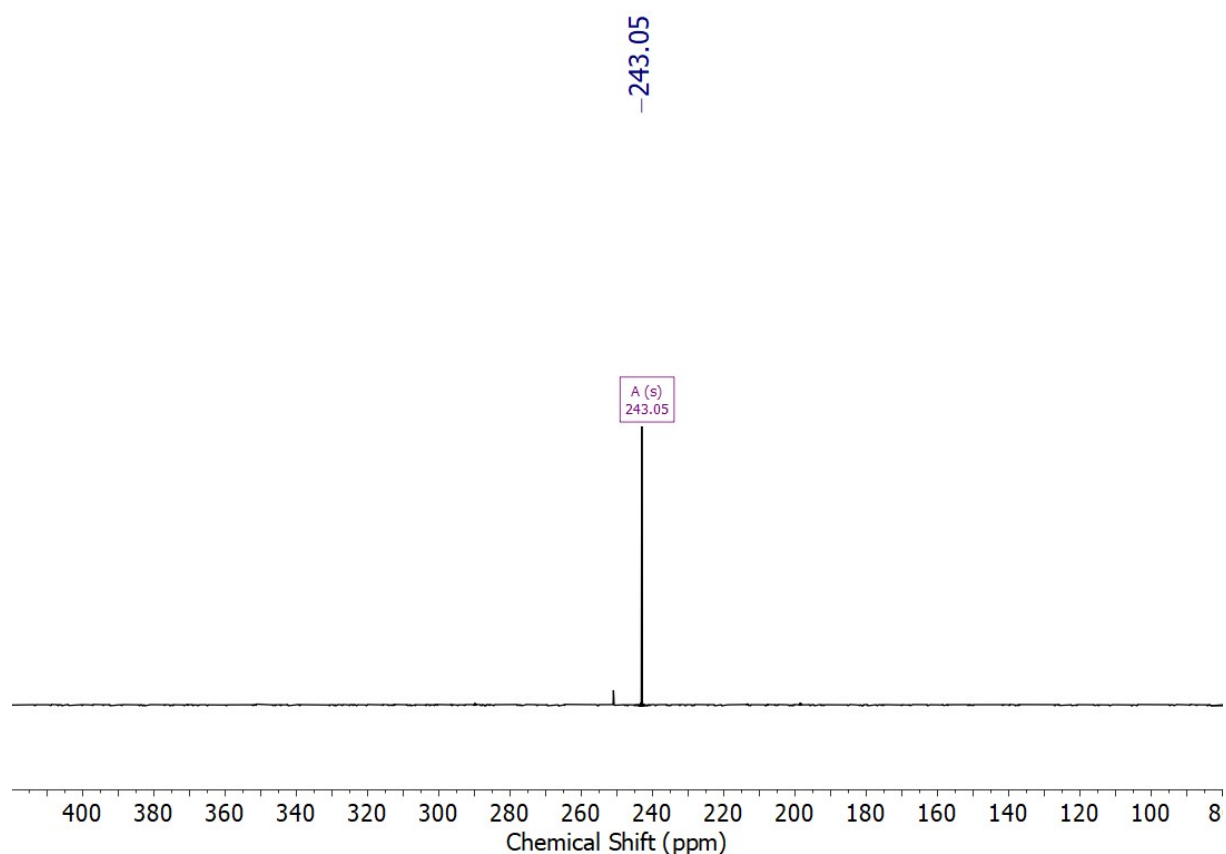
Figure S22. ^{31}P{^{1}H} NMR spectrum of **11** (thf-d_8, 162 MHz, rt).
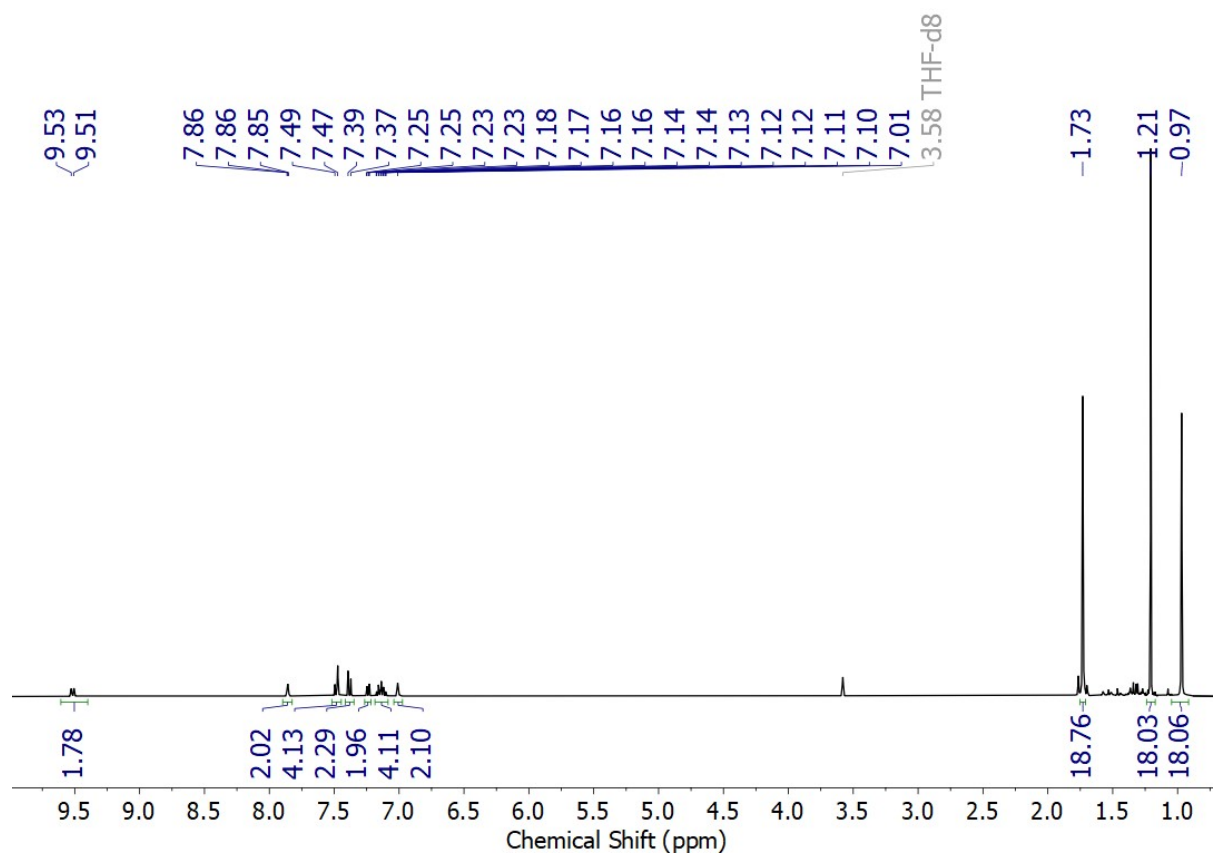
Figure S23. ^{1}H NMR spectrum of **11** (thf-d$_8$, 400 MHz, rt).
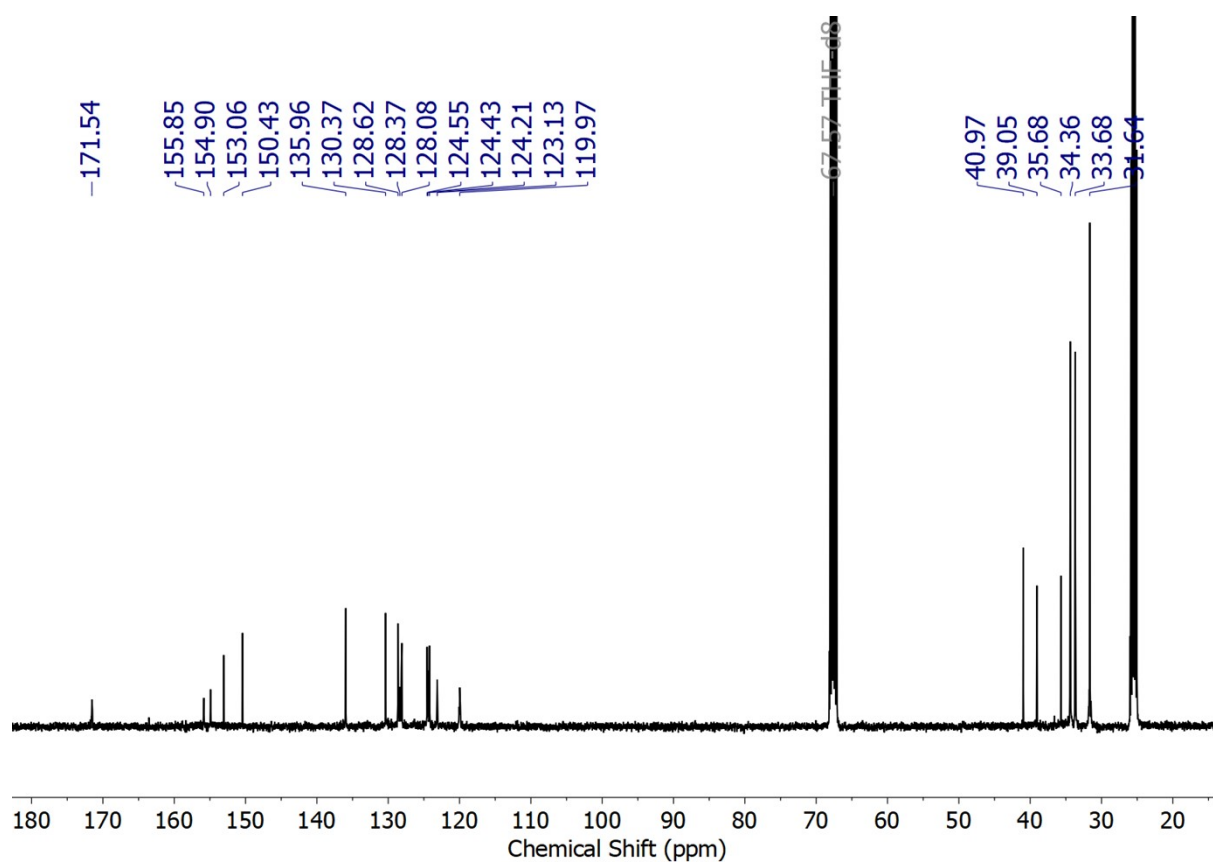
Figure S24. ^{13}C NMR spectrum of **11** (thf-d$_8$, 101 MHz, rt).

3.8. Thermal conversion of complex 6 and 7 into complex 8.
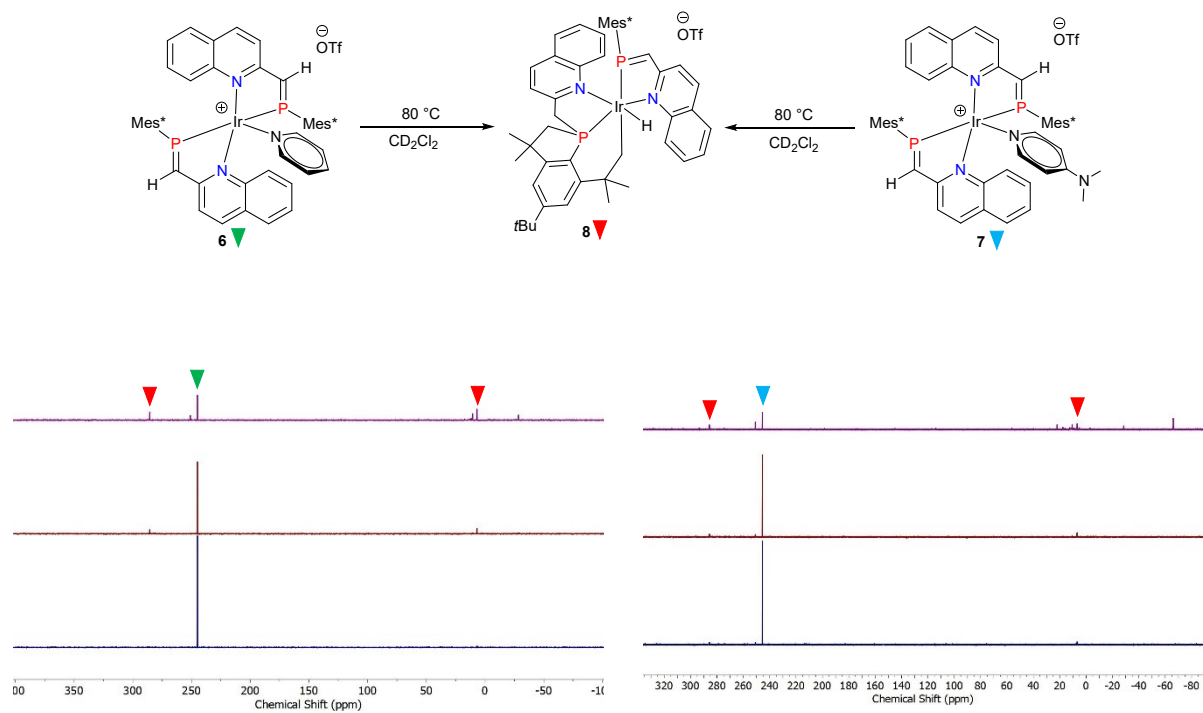
Figure S25. Reaction monitoring of complex **6** (right) and complex **7** (left) upon heating at 80 °C via $^{31}P\{^{1}H\}$ NMR spectroscopy (CD$_2$Cl$_2$, 162 MHz, rt).

4   CATALYTIC STUDIES

4.1. *N*-alkylation of aniline with benzyl alcohol catalysed by 5 and 6.

Benzyl alcohol (103 µL, 1.0 mmol), aniline (91 µL, 1.0 mmol), and thf (0.3 mL) were added to a Schlenk tube containing **5** or **6** (**5** 10.62 mg, 0.01 mmol; **6** 12.55 mg, 0.01 mmol) and KO*t*Bu (33.67 mg, 0.30 mmol). The solution was stirred at 100 °C for 24 h. The reaction progress and product yield were determined by GCMS using anisole as an internal standard. The GC-MS analysis of the resulting solution revealed the formation of *N*-benzylaniline. (**5** 0.90 mmol, 90%; **6** 0.53 mmol, 53%). The reaction products are known compounds.
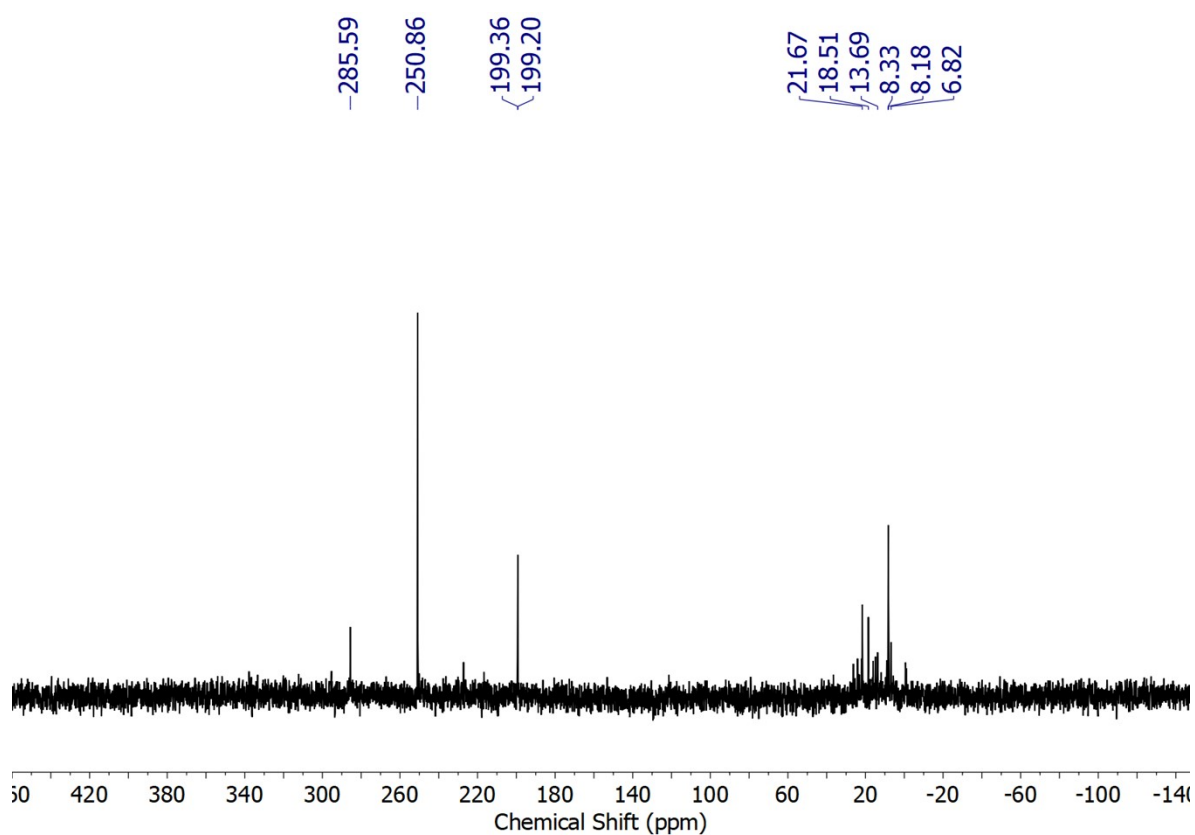
Figure S26. $^{31}P\{^1H\}$ NMR of reaction of complex **5** (0.010 g) with an excess of NaOEt (CD$_2$Cl$_2$, 162 MHz, 298 K).
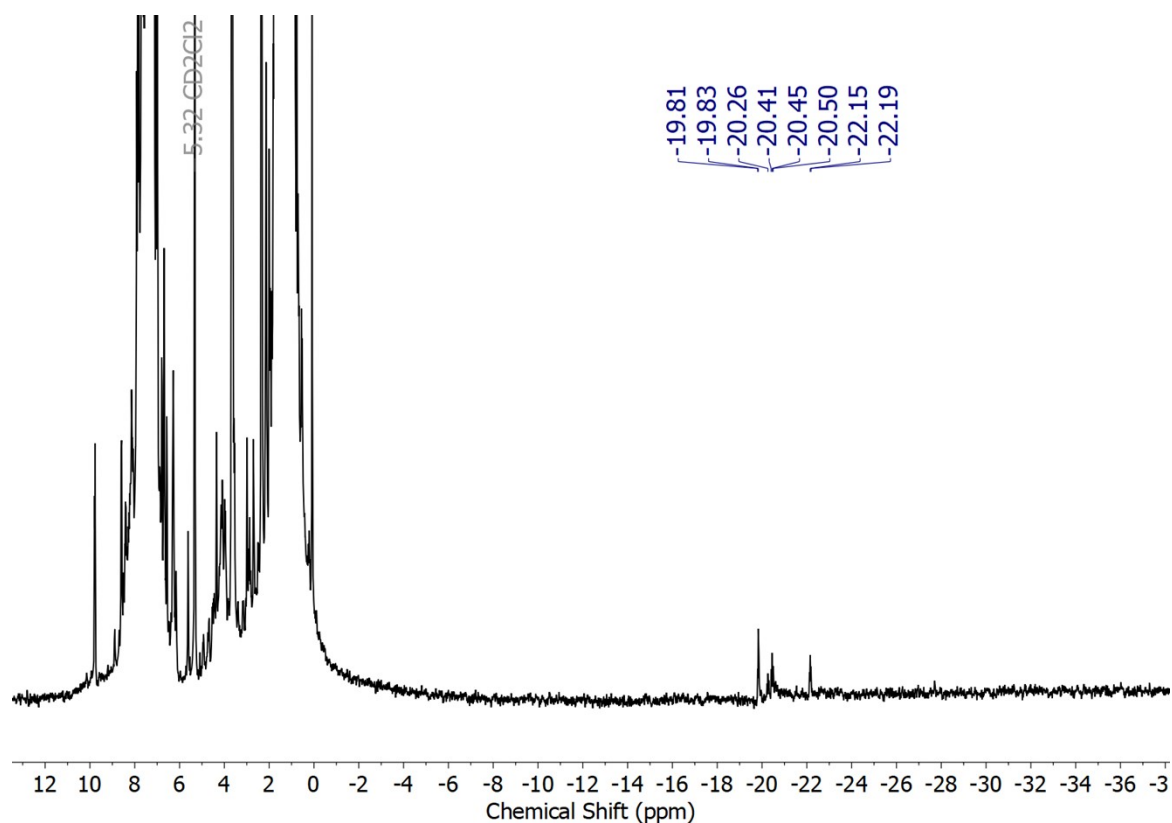
Figure S27. ^{1}H NMR spectrum of reaction of complex **5** (0.010 g) with an excess of NaOEt (CD$_2$Cl$_2$, 400 MHz, 298 K).

4.2. Upgrading of ethanol and methanol to isobutanol catalysed by 5.

An oven-dried 65 ml autoclave equipped with a fitted PTFE sleeve was charged with catalyst **5** (entries in Table 2), NaOMe (1.38 g, 25.54 mmol, 200 mol%), a magnetic stir bar and sealed. After evacuating the autoclave, EtOH (0.75 mL, 12.8 mmol) and MeOH (7.5 mL, excess) were added against a flow of nitrogen. The autoclave was sealed then placed into a pre-heated (180 °C) aluminium heating mantle with stirring set to 500 rpm. Upon completion, the autoclave was cooled to room temperature in an ice-water bath, after which any residual pressure was released from the autoclave. A sample of the reaction mixture (0.5 mL) was filtered through a short plug of acidic alumina before analysis by GC (100 μL of sample, 10 μL of hexadecane as internal standard and 1.7 mL Et$_2$O).

5   COMPUTATIONAL DETAILS

Computations were carried out using Gaussian16,[8] and MultiWfn 3.8.[9]

DFT structure optimisations using analytic gradients were performed using Gaussian16 and employed the hybrid exchange-correlation functional B3LYP[10] in conjunction with Grimme's dispersion correction D3(BJ)[11] and the def2-SVPP basis set[12] (notation B3LYP-D3/def2-SVPP). All structures were fully optimised and confirmed as minima or transition states by analytic frequency analyses.
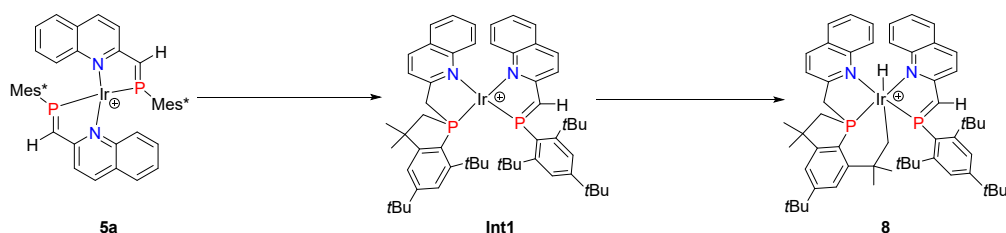
Scheme S1. Stepwise C-H activation at Ir(I).

Table S1. Summary of thermodynamic data of all calculated compounds used for thermodynamic calculations.

Complex	Nimag	SCF	H_{tot} [a.u.]	G_{tot} [a.u.]
5a	0	-3072.1942243	-3070.982541	-3071.139518
Int1	0	-3072.2563410	-3071.044315	-3071.200227
8	0	-3072.2534894	-3071.043882	-3071.200064

UV-vis absorption spectra were calculated with Gaussian16 using the TD-DFT method[13] at the B3LYP-D3/def2-SVPP level of theory (using the B3LYP-D3/ def2-SVPP geometries, *vide supra*). For the visualization of the charge density difference between the ground state and selected excited states we used MultiWfn 3.8 employing Gaussian16 formatted checkpoint files (see Figure 4).

5.1 Comparison of the experimental and calculated UV/Vis spectra of complex 5, 6, 7, 8, 9 and 10.

These calculations were performed to gain a deeper understanding about the colour of the herein described complexes. The calculations were performed on the former described B3LYP-D3(BJ)/ def2-SVPP level of theory considering 40 excited states as well as the scrf approach for dichloromethane as solvent. The calculated data were plotted with a half-width of 2000 cm^{-1} and normalised to a prominent band of the experimentally observed spectrum. For the experimental measurement of the UV/Vis spectra of complexes, we diluted approximately 1 mg of complex in 5 mL dichloromethane under an Argon atmosphere.

Figure S28: Plot of the UV/Vis spectra and the calculated oscillator strength of complex **5**.
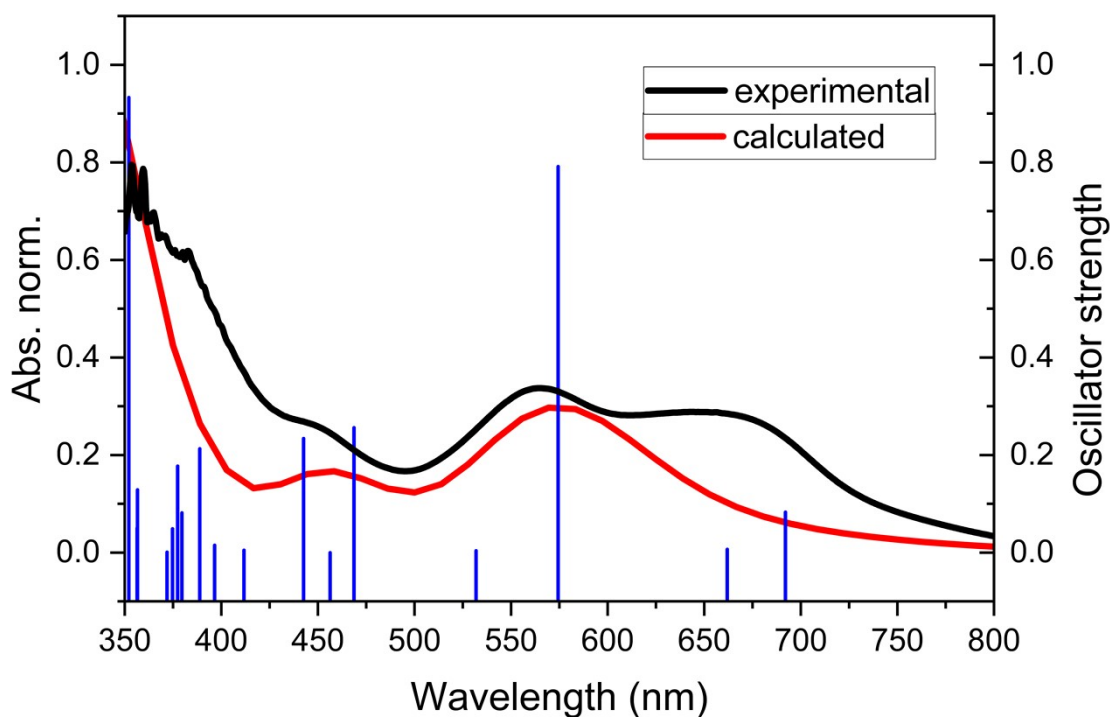
Figure S29: Plot of the UV/Vis spectra and the calculated oscillator strength of complex **6**.
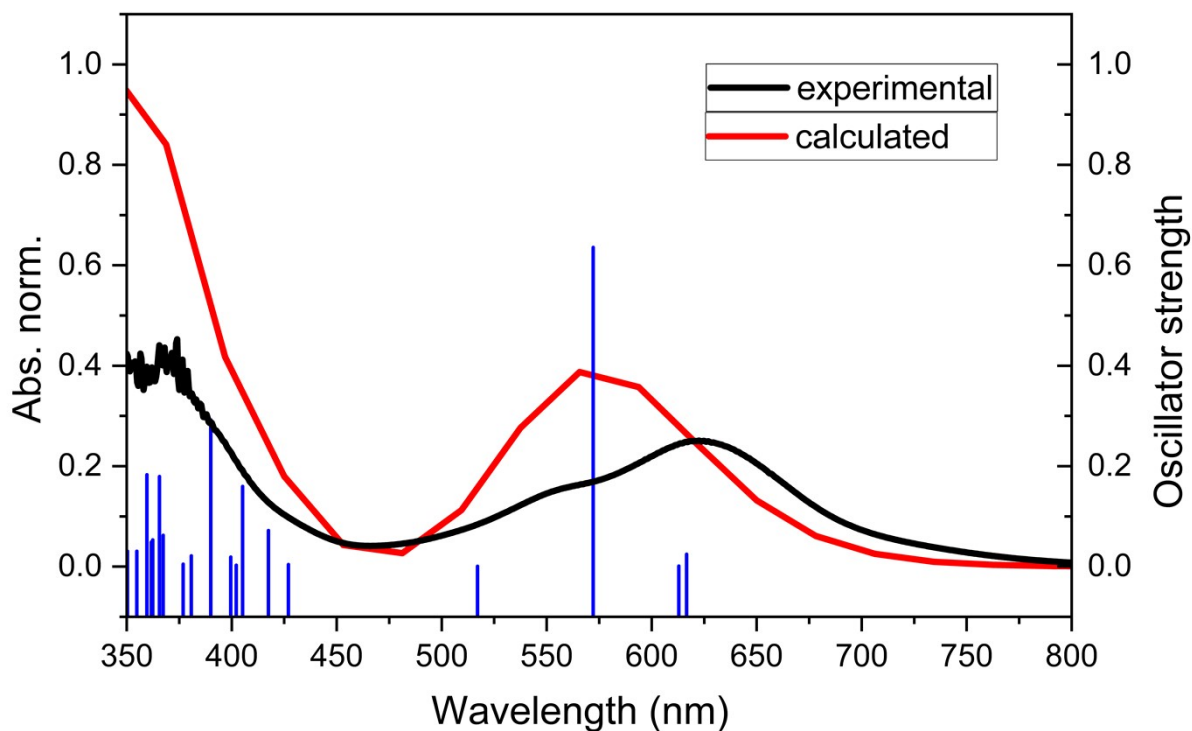
Figure S30: Plot of the UV/Vis spectra and the calculated oscillator strength of complex **7**.
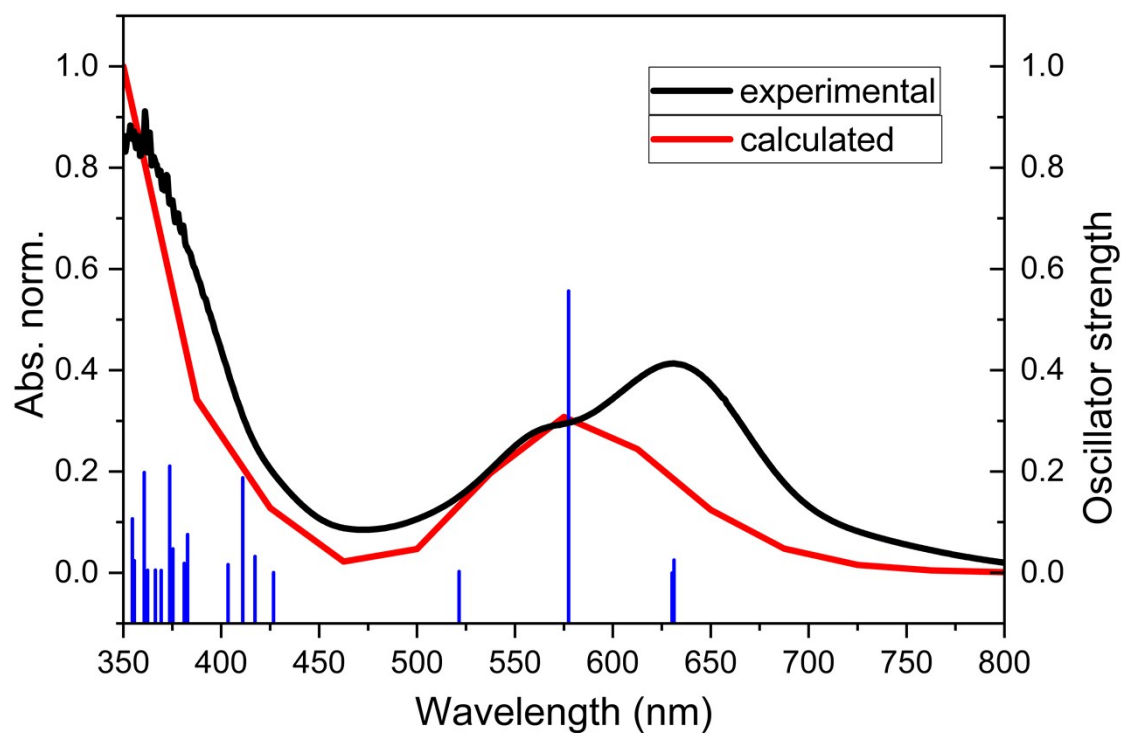
Figure S31: Plot of the UV/Vis spectra and the calculated oscillator strength of complex **8**.
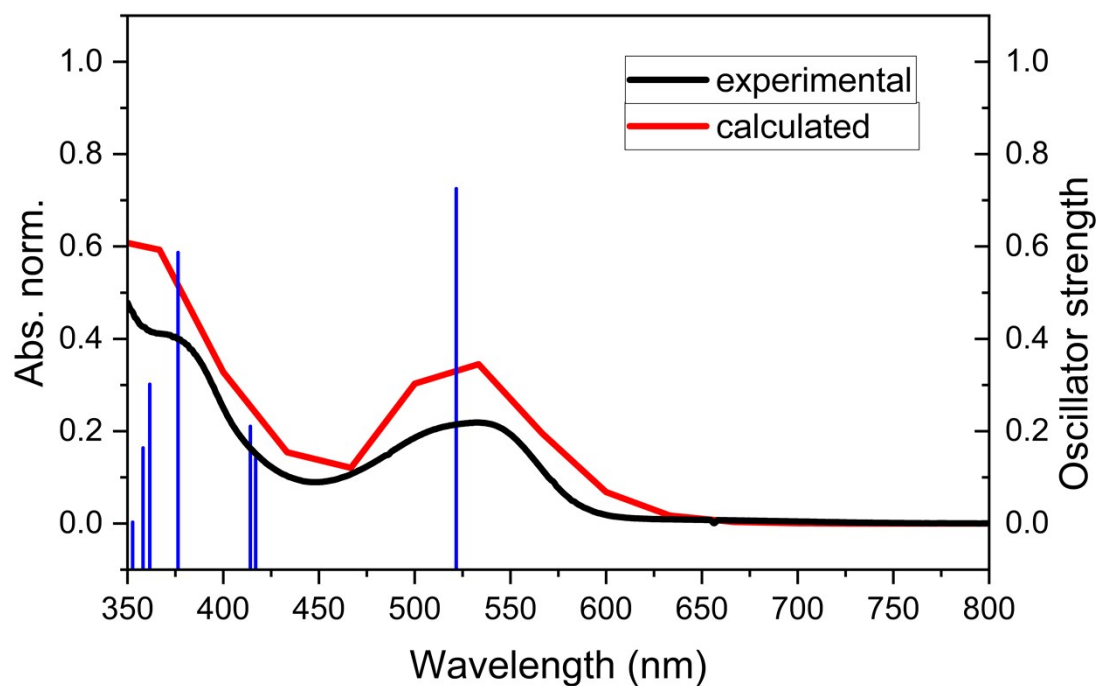
Figure S32: Plot of the UV/Vis spectra and the calculated oscillator strength of complex **9**.
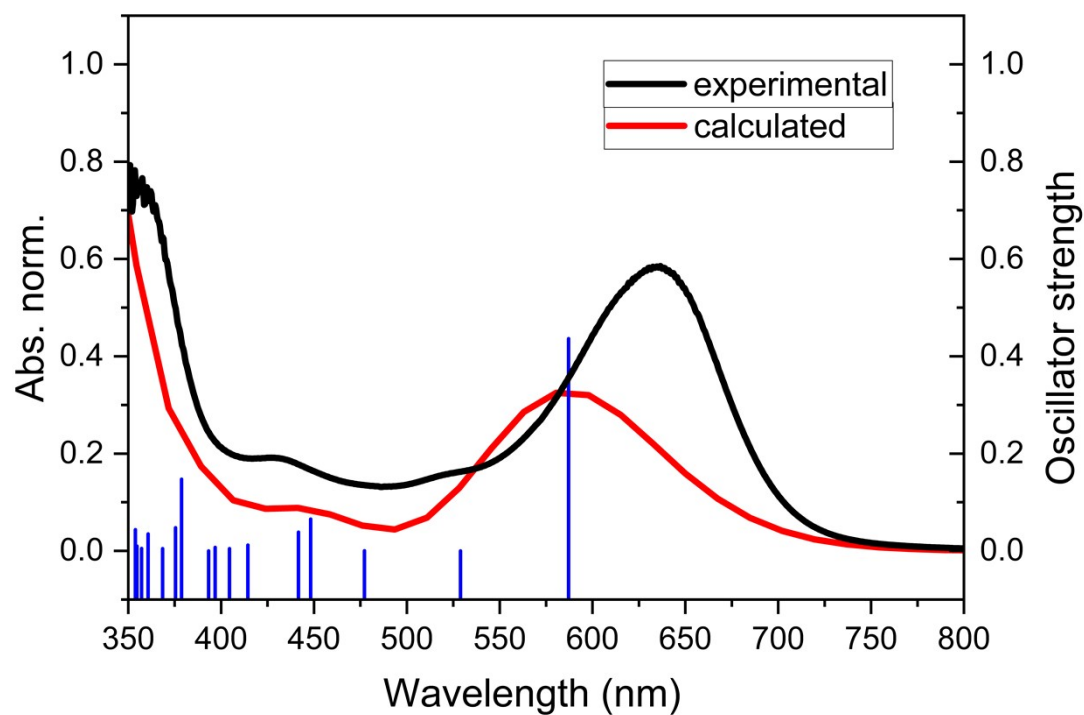
Figure S33: Plot of the UV/Vis spectra and the calculated oscillator strength of complex **10**.
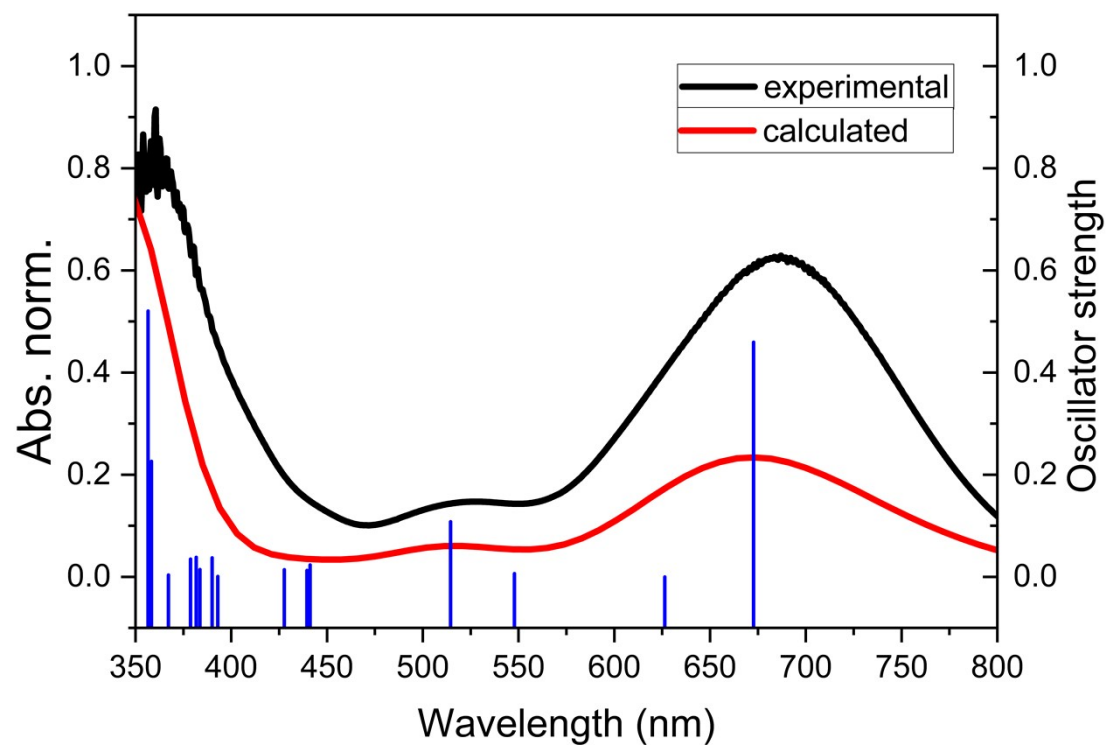
5.2 Report of the first 10 excited states of complex 5 and corresponding charge density difference diagrams

IrPNCl_TD_UV_NEW

----

b3lyp empiricaldispersion=gd3bj def2svpp geom=allcheck guess=read TD

=(Nstates=40) scrf=(pcm,solvent=dichloromethane)

Excitation energies and oscillator strengths:

Excited State   1:   Singlet-A   1.7916 eV 692.04 nm f=0.0169 <S**2>=0.000

   243 -> 245   0.69229

This state for optimization and/or second-order correction.

Total Energy, E(TD-HF/TD-DFT) = -3532.44000540

Copying the excited state density for this state as the 1-particle RhoCI density.

Excited State   2:   Singlet-A   1.8731 eV 661.91 nm f=0.0014 <S**2>=0.000

   242 -> 245   -0.27944

   243 -> 244   0.64071

Excited State   3:   Singlet-A   2.1585 eV 574.40 nm f=0.1610 <S**2>=0.000

   241 -> 245   -0.10602

   242 -> 244   0.68689

Excited State   4:   Singlet-A   2.3310 eV 531.88 nm f=0.0008 <S**2>=0.000

   241 -> 244   -0.15086

   242 -> 245   0.62020

   243 -> 244   0.26780

Excited State   5:   Singlet-A   2.6453 eV 468.70 nm f=0.0521 <S**2>=0.000

   239 -> 245   -0.14166

   241 -> 245   0.64322

Excited State   6:   Singlet-A   2.7172 eV 456.29 nm f=0.0000 <S**2>=0.000

   241 -> 244   0.65465

   242 -> 245   0.11037

   243 -> 247   -0.11134

Excited State   7:   Singlet-A   2.8016 eV 442.55 nm f=0.0476 <S**2>=0.000

   243 -> 246   0.65875

Excited State   8:   Singlet-A   3.0115 eV 411.71 nm f=0.0010 <S**2>=0.000

   242 -> 246   0.65748

   243 -> 247   -0.17050

Excited State   9:   Singlet-A   3.1268 eV 396.52 nm f=0.0031 <S**2>=0.000

   239 -> 244   0.13638

   240 -> 245   -0.23502

   242 -> 245   0.10040

   242 -> 246   0.12431

   243 -> 247   0.61318

Excited State 10:   Singlet-A   3.1888 eV 388.81 nm f=0.0433 <S**2>=0.000

   240 -> 244   0.18479

   242 -> 247   -0.17134

   243 -> 248   0.64563

5.3 Report of the first 10 excited states of complex 6 and corresponding charge density difference diagrams

Ir-pyridine_TD_UV

----

b3lyp empiricaldispersion=gd3bj def2svpp geom=allcheck guess=read TD

=(Nstates=40) scrf=(pcm,solvent=dichloromethane)

Excitation energies and oscillator strengths:

Excited State   1:   Singlet-A   2.0107 eV 616.63 nm f=0.0074 <S**2>=0.000

    254 -> 257   0.67247

    255 -> 256   0.19118

This state for optimization and/or second-order correction.

Total Energy, E(TD-HF/TD-DFT) = -3320.32396611

Copying the excited state density for this state as the 1-particle RhoCI density.

Excited State   2:   Singlet-A   2.0229 eV 612.89 nm f=0.0003 <S**2>=0.000

    254 -> 256   0.61593

    255 -> 257   0.33116

Excited State   3:   Singlet-A   2.1670 eV 572.16 nm f=0.1902 <S**2>=0.000

    254 -> 257   -0.18840

    255 -> 256   0.67242

Excited State   4:   Singlet-A   2.3979 eV 517.04 nm f=0.0002 <S**2>=0.000

    254 -> 256   -0.32935

    255 -> 257   0.60972

Excited State   5:   Singlet-A   2.9038 eV 426.97 nm f=0.0013 <S**2>=0.000

```
245 -> 256      0.10204

253 -> 256      0.67201

255 -> 259     -0.11907


Excited State   6:      Singlet-A      2.9697 eV  417.50 nm  f=0.0215  <S**2>=0.000

245 -> 257      0.13664

249 -> 257      0.10300

251 -> 257      0.10310

253 -> 257      0.61654

254 -> 259     -0.21542


Excited State   7:      Singlet-A      3.0602 eV  405.15 nm  f=0.0478  <S**2>=0.000

251 -> 257      0.11752

253 -> 257      0.12913

254 -> 259      0.60407

254 -> 265      0.11157

255 -> 258      0.18014


Excited State   8:      Singlet-A      3.0831 eV  402.15 nm  f=0.0009  <S**2>=0.000

253 -> 256      0.10516

255 -> 259      0.66003

255 -> 265      0.10562

255 -> 267      0.10092


Excited State   9:      Singlet-A      3.1030 eV  399.56 nm  f=0.0057  <S**2>=0.000

254 -> 259     -0.13811

255 -> 258      0.66442

255 -> 260      0.14300
```

Excited State 10:   Singlet-A   3.1790 eV 390.01 nm f=0.0875 <S**2>=0.000

    254 -> 258   0.68361

5.4 Report of the first 10 excited states of complex 7 and corresponding charge density difference diagrams

Ir-DMAP_TD_UV

 # b3lyp empiricaldispersion=gd3bj def2svpp geom=allcheck guess=read TD

 =(Nstates=40) scrf=(pcm,solvent=dichloromethane)

Excitation energies and oscillator strengths:

 Excited State 1:   Singlet-A   1.9640 eV 631.28 nm f=0.0088 <S**2>=0.000

    266 -> 268   -0.15956

    267 -> 269   0.67532

This state for optimization and/or second-order correction.

Total Energy, E(TD-HF/TD-DFT) = -3454.21491759

Copying the excited state density for this state as the 1-particle RhoCI density.

 Excited State 2:   Singlet-A   1.9672 eV 630.27 nm f=0.0002 <S**2>=0.000

    266 -> 269   -0.29338

    267 -> 268   0.63080

 Excited State 3:   Singlet-A   2.1474 eV 577.36 nm f=0.1884 <S**2>=0.000

    266 -> 268   0.68073

    267 -> 269   0.15757

 Excited State 4:   Singlet-A   2.3776 eV 521.47 nm f=0.0011 <S**2>=0.000

    266 -> 269   0.62822

267 -> 268   0.29447

Excited State   5:   Singlet-A   2.9059 eV 426.66 nm f=0.0004 <S**2>=0.000
   265 -> 268   0.66933
   266 -> 270   0.11480

Excited State   6:   Singlet-A   2.9715 eV 417.25 nm f=0.0112 <S**2>=0.000
   265 -> 269   -0.46631
   267 -> 270   0.49041

Excited State   7:   Singlet-A   3.0167 eV 410.99 nm f=0.0637 <S**2>=0.000
   256 -> 269   0.11833
   262 -> 269   -0.10370
   263 -> 268   0.10412
   264 -> 269   0.14714
   265 -> 269   0.41207
   266 -> 271   0.11285
   267 -> 270   0.43805

Excited State   8:   Singlet-A   3.0731 eV 403.45 nm f=0.0057 <S**2>=0.000
   265 -> 268   -0.10200
   266 -> 270   0.66826
   266 -> 277   0.10671
   266 -> 279   0.10103

Excited State   9:   Singlet-A   3.2393 eV 382.75 nm f=0.0258 <S**2>=0.000
   262 -> 268   -0.20006
   263 -> 269   -0.21520
   264 -> 268   0.22269

267 -> 271   0.57913

Excited State 10:   Singlet-A   3.2537 eV 381.05 nm f=0.0065 <S**2>=0.000

    262 -> 269   0.10836

    263 -> 268   0.53637

    264 -> 269   -0.16636

    266 -> 271   -0.33403

    267 -> 272   0.19760

5.5   Report of the first 10 excited states of complex 8 and corresponding charge density difference diagrams

Ir-Hydrido_TD_UV

 # b3lyp empiricaldispersion=gd3bj def2svpp geom=allcheck guess=read TD

 =(Nstates=40) scrf=(pcm,solvent=dichloromethane)

Excitation energies and oscillator strengths:

 Excited State   1:   Singlet-A   2.3767 eV 521.68 nm f=0.1357 <S**2>=0.000

    234 -> 235   0.69680

This state for optimization and/or second-order correction.

 Total Energy, E(TD-HF/TD-DFT) = -3072.20795400

Copying the excited state density for this state as the 1-particle RhoCI density.

 Excited State   2:   Singlet-A   2.9738 eV 416.92 nm f=0.0270 <S**2>=0.000

    225 -> 235   -0.10034

    233 -> 235   0.64861

    234 -> 236   0.13117

Excited State   3:   Singlet-A   2.9936 eV 414.16 nm f=0.0398 <S**2>=0.000
    233 -> 235   -0.10412
    234 -> 236   0.68764

Excited State   4:   Singlet-A   3.2940 eV 376.40 nm f=0.1099 <S**2>=0.000
    230 -> 235   -0.15402
    231 -> 235   0.11683
    232 -> 235   0.61957
    233 -> 235   0.12421
    234 -> 237   0.15246

Excited State   5:   Singlet-A   3.4286 eV 361.62 nm f=0.0568 <S**2>=0.000
    226 -> 235   0.15802
    227 -> 235   -0.15023
    228 -> 235   -0.11633
    229 -> 235   -0.29724
    230 -> 235   0.25577
    231 -> 235   0.48020
    233 -> 235   0.15799

Excited State   6:   Singlet-A   3.4619 eV 358.14 nm f=0.0311 <S**2>=0.000
    224 -> 235   -0.23839
    226 -> 235   0.21309
    227 -> 235   -0.34884
    229 -> 235   0.46405
    230 -> 235   0.21664

Excited State   7:   Singlet-A   3.5155 eV 352.68 nm f=0.0012 <S**2>=0.000
    227 -> 235   -0.11974

228 -> 235   0.66189

  229 -> 235   -0.15180

 Excited State   8:   Singlet-A   3.5537 eV 348.89 nm f=0.0027 <S**2>=0.000

   229 -> 235   -0.26191

   230 -> 235   0.43404

   231 -> 235   -0.41181

   232 -> 235   0.22825

 Excited State   9:   Singlet-A   3.5866 eV 345.68 nm f=0.0164 <S**2>=0.000

   224 -> 235   0.17285

   226 -> 235   -0.17286

   227 -> 235   0.35045

   228 -> 235   0.18378

   229 -> 235   0.28607

   230 -> 235   0.35998

   231 -> 235   0.20833

   234 -> 237   -0.11655

 Excited State 10:   Singlet-A   3.6284 eV 341.70 nm f=0.0044 <S**2>=0.000

   233 -> 236   0.66158

   234 -> 237   -0.20270

5.6 Report of the first 10 excited states of complex 9 and corresponding charge density difference diagrams

IrPNCO_TD_UV

----

b3lyp empiricaldispersion=gd3bj def2svpp geom=allcheck guess=read TD

=(Nstates=40) scrf=(pcm,solvent=dichloromethane)

Excitation energies and oscillator strengths:

Excited State   1:   Singlet-A   2.1118 eV 587.10 nm f=0.2256 <S**2>=0.000

    241 -> 242   0.70012

This state for optimization and/or second-order correction.

Total Energy, E(TD-HF/TD-DFT) = -3185.43401120

Copying the excited state density for this state as the 1-particle RhoCI density.

Excited State   2:   Singlet-A   2.3441 eV 528.91 nm f=0.0002 <S**2>=0.000

    240 -> 242   0.64342

    241 -> 243   0.27280

Excited State   3:   Singlet-A   2.5982 eV 477.19 nm f=0.0004 <S**2>=0.000

    239 -> 242   0.19230

    240 -> 242   -0.25216

    241 -> 243   0.61939

Excited State   4:   Singlet-A   2.7662 eV 448.21 nm f=0.0341 <S**2>=0.000

    239 -> 243   0.11515

    240 -> 243   0.68011

Excited State   5:   Singlet-A   2.8074 eV 441.64 nm f=0.0201 <S**2>=0.000

    239 -> 242   0.67043

    241 -> 243   -0.16753

Excited State   6:   Singlet-A   2.9916 eV 414.44 nm f=0.0064 <S**2>=0.000

    238 -> 242   0.68323

    239 -> 243   -0.13301

Excited State   7:   Singlet-A   3.0650 eV 404.52 nm f=0.0027 <S**2>=0.000

   237 -> 242   0.69362

Excited State   8:   Singlet-A   3.1248 eV 396.78 nm f=0.0040 <S**2>=0.000

   236 -> 242   0.66078

   239 -> 243   -0.21187

Excited State   9:   Singlet-A   3.1528 eV 393.25 nm f=0.0002 <S**2>=0.000

   241 -> 245   0.66256

   241 -> 248   0.12851

Excited State 10:   Singlet-A   3.2744 eV 378.65 nm f=0.0764 <S**2>=0.000

   233 -> 242   -0.10124

   235 -> 242   -0.17573

   236 -> 242   0.15723

   239 -> 243   0.59027

   240 -> 243   -0.10269

   240 -> 245   0.13090

   241 -> 244   -0.15608

5.7   Report of the first 10 excited states of complex 10 and corresponding charge density difference diagrams

IrPNCH3_TD_UV

----

b3lyp empiricaldispersion=gd3bj def2svpp geom=allcheck guess=read TD

=(Nstates=40) scrf=(pcm,solvent=dichloromethane)

Excitation energies and oscillator strengths:

Excited State   1:   Singlet-A   1.8430 eV 672.73 nm f=0.1725 <S**2>=0.000

   239 -> 240   0.69692

This state for optimization and/or second-order correction.

Total Energy, E(TD-HF/TD-DFT) = -3112.18599625

Copying the excited state density for this state as the 1-particle RhoCI density.

Excited State   2:   Singlet-A   1.9794 eV 626.38 nm f=0.0009 <S**2>=0.000

   238 -> 240   0.55039

   239 -> 241   -0.42948

Excited State   3:   Singlet-A   2.2630 eV 547.87 nm f=0.0033 <S**2>=0.000

   238 -> 240   0.42242

   239 -> 241   0.54324

Excited State   4:   Singlet-A   2.4097 eV 514.53 nm f=0.0412 <S**2>=0.000

   238 -> 241   0.68579

Excited State   5:   Singlet-A   2.8106 eV 441.14 nm f=0.0097 <S**2>=0.000

   236 -> 240   0.12241

   237 -> 240   -0.34365

   239 -> 242   0.56460

   239 -> 243   0.15018

Excited State   6:   Singlet-A   2.8212 eV 439.48 nm f=0.0056 <S**2>=0.000

   236 -> 240   0.12136

   237 -> 240   0.49003

   239 -> 242   0.37435

239 -> 243   -0.25664

Excited State   7:   Singlet-A   2.8991 eV 427.66 nm f=0.0061 <S**2>=0.000
    237 -> 240   0.29019
    239 -> 243   0.62462

Excited State   8:   Singlet-A   3.1550 eV 392.97 nm f=0.0012 <S**2>=0.000
    236 -> 240   -0.17431
    238 -> 242   -0.24308
    239 -> 244   0.61191

Excited State   9:   Singlet-A   3.1794 eV 389.96 nm f=0.0148 <S**2>=0.000
    236 -> 240   0.55999
    237 -> 241   0.24196
    238 -> 243   0.20000
    239 -> 242   -0.10736
    239 -> 244   0.16068
    239 -> 245   0.12191

Excited State 10:   Singlet-A   3.2317 eV 383.65 nm f=0.0063 <S**2>=0.000
    237 -> 241   -0.42361
    238 -> 243   0.48233
    238 -> 244   -0.13061
    239 -> 245   0.11583

6 REFERENCES

1   P. Gupta, T. Taeufer, J.-E. Siewert, F. Reiß, H.-J. Drexler, J. Pospech, T. Beweries and C. Hering-Junghans, Synthesis, Coordination Chemistry, and Mechanistic Studies of P,N-Type Phosphaalkene-Based Rh(I) Complexes, *Inorg. Chem.*, 2022, **61**, 11639-11650.

2   R. I. Yousef, B. Walfort, T. Rüffer, C. Wagner, H. Schmidt, R. Herzog and D. Steinborn, Synthesis, characterization and Schlenk equilibrium studies of methylmagnesium compounds with O-and N-donor ligands–the unexpected behavior of [MgMeBr (pmdta)](pmdta= N, N, N', N ", N "-pentamethyldiethylenetriamine), *J. Organomet. Chem.*, 2005, **690**, 1178-1191.

3   G. M. Sheldrick, SHELXT–Integrated space-group and crystal-structure determination, *Acta Cryst. Section A: Foundations and Advances*, 2015, **71**, 3-8.

4   G. M. Sheldrick, Program for the solution of crystal structures, *SHELXL-97.*, 1997.

5   G. M. Sheldrick, Crystal structure refinement with SHELXL, *Acta Cryst. Section C: Structural Chemistry*, 2015, **71**, 3-8.

6   G. M. Sheldrick, SADABS Version 2, University of Göttingen, Germany, 2004.

7   A. L. Spek, Structure validation in chemical crystallography, *Acta Crystallogr. Sect. D. Biol. Crystallogr.*, 2009, **65**, 148-155.

8   Frisch, M. J.; Trucks, G. W.; Schlegel, H. B.; Scuseria, G. E.; Robb, M. A.; Cheeseman, J. R.; Scalmani, G.; Barone, V.; Mennucci, B.; Peterson, G. A.; Nakatsuji, H.; Caricato, M.; Li, X.; Hratchian, H. P.; Izmaylov, A. F.; Bloino, J.; Zheng, G.; Sonnenberg, J. L.; Hada, M.; Ehara, M.; Toyota, K.; Fukuda, R.; Hasegawa, J.; Ishida, M.; Nakajima, T.; Honda, Y.; Kitao, O.; Nakai, H.; Vreven, T.; Montgomery Jr., J. A.; Peralta, J. E.; Ogliaro, F.; Bearpark, M.; Heyd, J. J.; Brothers, E.; Kudin, K. N.; Staroverov, V. N.; Keith, T.; Kobayashi, R.; Normand, J.; Raghavachari, K.; Rendell, A.; Burant, J. C.; Iyengar, S. S.; Tomasi, J.; Cossi, M.; Rega, N.; Millam, J. M.; Klene, M.; Know, J. E.; Cross, J. B.; Bakken, V.; Adamo, C.; Jaramillo, J.; Gomperts, R.; Stratmann, R. E.; Yazyev, O.; Austin, A. J.; Cammi, R.; Pomelli, C.; Ochterski, J. W.; Martin, R. L.; Morokuma, K.; Zakrezewski, V. G.; Voth, G. A.; Salvador, P.; Dannenberg, J. J.; Dapprich, S.; Daniels, A. D.; Farkas, O.; Foresman, J. B.; Ortiz, J. V.; Cioslowski, J.; Fox, D. J. Gaussian 09, Revision E.01. Gaussian Inc.: Wallingford CT 2013.

9   T. Lu and F. Chen, Multiwfn: A Multifunctional Wavefunction Analyzer. *J. Comput. Chem.* 2012, **33**, 580–592.

10   (a)   S. H. Vosko, L. Wilk and M. Nusair, Accurate Spin-Dependent Electron Liquid
Correlation Energies for Local Spin Density Calculations: A Critical Analysis. *Can. J.
Phys.* 1980, **58**, 1200–1211; (b) C. Lee, W. Yang and R. G. Parr, Development of the
Colle-Salvetti Correlation-Energy Formula into a Functional of the Electron Density.
Phys. Rev. B 1988, **37**, 785–789; (c) A. D. Becke, Density-Functional Exchange-Energy
Approximation with Correct Asymptotic Behavior. *Phys. Rev. A* 1988, **38**, 3098–3100;
(d) B. Miehlich, A. Savin, H. Stoll and H. Preuss, Results Obtained with the Correlation
Energy Density Functionals of Becke and Lee, Yang and Parr. *Chem. Phys. Lett.* 1989,
157, 200–206; (e) A. D. Becke, Density-functional Thermochemistry. III. The Role of
Exact Exchange. *J. Chem. Phys.* 1993, **98**, 5648–5652; (f) P. J. Stephens, F. J. Devlin, C. F.
Chabalowski and M. J. Frisch, Ab Initio Calculation of Vibrational Absorption and
Circular Dichroism Spectra Using Density Functional Force Fields. *J. Phys. Chem.* 1994,
98, 11623–11627.

11   (a) S. Grimme, J. Antony, S. Ehrlich and H. A. Krieg, Consistent and Accurate Ab Initio
Parametrization of Density Functional Dispersion Correction (DFT-D) for the 94
Elements H-Pu. *J. Chem. Phys.* 2010, **132**, 154104; (b) S. Grimme, S. Ehrlich and L.
Goerigk, Effect of the Damping Function in Dispersion Corrected Density Functional
Theory. *J. Comput. Chem.* 2011, **32**, 1456–1465.

12   F. Weigend and R. Ahlrichs, Balanced Basis Sets of Split Valence, Triple Zeta Valence
and Quadruple Zeta Valence Quality for H to Rn: Design and Assessment of Accuracy.
Phys. Chem. Chem. Phys. 2005, **7**, 3297–3305.

13   (a) R. Bauernschmitt and R. Ahlrichs, Treatment of Electronic Excitations within the
Adiabatic Approximation of Time Dependent Density Functional Theory. *Chem. Phys.
Lett.* 1996, **256**, 454–464; (b) R. E. Stratmann, G. E. Scuseria and M. J. Frisch, An
Efficient Implementation of Time-Dependent Density-Functional Theory for the
Calculation of Excitation Energies of Large Molecules. *J. Chem. Phys.* 1998, **109**, 8218–
8224; (c) M. E. Casida, C. Jamorski, K. C.; Casida and D. R. Salahub, Molecular Excitation
Energies to High-Lying Bound States from Time-Dependent Density-Functional
Response Theory: Characterization and Correction of the Time-Dependent Local
Density Approximation Ionization Threshold. *J. Chem. Phys.* 1998, **108**, 4439–4449.